GOSPODARKA SUROWCAMI MINERALNYMI – MINERAL RESOURCES MANAGEMENT

2023 Volume 39 Issue 2 Pages 37–69

DOI: 10.24425/gsm.2023.145889

SEMA TETIKER[1]

Mineralogy and geochemistry of Upper Cretaceous Mazıdağı Phosphorite Deposits from the Northern Arabian Plate (Mardin, Turkey)

Introduction

Marine phosphate rocks are biochemical rocks rich in phosphorus process with a P_2O_5 content of more than 18% (Boggs 2009). Phosphate minerals, which are utilsed in many fields, are widely exploited in the fertilizer (90%) and chemical (10%) industries (Lauriente 1996). Generally, phosphorite deposits are not primarily formed under marine conditions. The deposition of sedimentary phosphates occurs when appropriate paleoceanographic, paleogeographic, paleoclimatic, and other physicochemical conditions occur simultaneously. Specifically, deposition requires that the water in shallow marine environments has the biological material and ion concentrations that re necessary for minerals to develop and reproduce (Orris and Chernoff 2004; Arning et al. 2009; Goldhammer et al. 2010; Brock and Schulz-Vogt 2011; Crosby and Bailey 2012; Daneshian et al. 2015; Mänd et al. 2018).

✉ Corresponding Author: Sema Tetiker; e-mail: sema.tetiker@batman.edu.tr
[1] Batman University, Turkey; ORCID iD: 0000-0001-5158-7364; e-mail: sema.tetiker@batman.edu.tr

Previous work has stated that sedimentary phosphate deposits primarily formed throughout the Cambrian, Permian, Jurassic, Cretaceous, Eocene and Miocene eras (Cook and McElhinny 1979). Phosphorite formations developed in many areas in the northern part of the Arabian Plate, which is associated with the evolution of the Tethys Sea, especially during the Cretaceous-Eocene period (Soudry et al. 2006). The Upper Cretaceous-Paleocene Mediterranean phosphorite belt, which extends from southwestern Turkey to Morocco, encompasses phosphorite deposits in Israel, Syria, Tunisia, Iraq, Saudi Arabia, Algeria, Egypt, Iran and Jordan (Figure 1) (Belayouni and Beja-Sassi 1987; Svoboda 1989; Soudry et al. 2002; Baioumy et al. 2007; Aba-Hussain et al. 2009; Abed 2013; Al-Hobaib et al. 2013; Abed et al. 2016; Kechiched et al. 2020; Salsani et al. 2020; El Bamiki et al. 2021; Ghasemian et al. 2022). Mazıdağı (Mardin) phosphate occurrences represent an eastern part of this belt associated with Tethys (Figure 1a).

The sedimentary phosphate deposits that form in marine environments are of great importance due to their high content of P and rare earth elements (average world phosphorites; AWP_{REEs} = 457.30 ppm). The abundance of REE in phosphates also provides important information about the physicochemical conditions of the paleoenvironment (Khan et al. 2012b; Kechidhed et al. 2020). Phosphorus generally behaves in a similar manner to REE elements during precipitation. Phosphates typically have high REE contents, show positive Eu and negative Ce anomalies because of the redox conditions and composition of the depositional environment (Altschuler et al. 1967; Altschuler, 1980; Khan et al. 2012b).

The average P_2O_5 mean of the Upper Cretaceous and Paleocene phosphorite deposits on the Mediterranean belt are as follows: 25.67 wt.% for Egypt (Abou El-Anwar et al. 2017), 25.00 wt.% for Israel (Soudry et al. 2012), 23.0 wt.% for Saudi Arabia (Meissner and Ankary 1970), 23.0 wt.% for Iran (Salsani et al. 2020), 26.53 wt.% for Algeria (Bezzi et al. 2012), 19.50 wt.% for Jordan (Abed et al. 2016), 22.00 wt.% for Morocco (El Bamiki et al. 2021), 22.67 wt.% for Tunisia (Gallala et al. 2016), and 22.0 wt.% for Iraq (Benni 2013). The average content of REEs for phosphorite in Mediterranean belt countries is very high, specifically, the content levels in these countries are as follows: 1810.5 ppm in Egypt, 35 ppm in Israel, 350 ppm in Saudi Arabia, 123.1 ppm in Iran, 713 ppm in Algeria, 187 ppm in Jordan, 571.75 ppm in Morocco, 400.3 ppm in Tunisia and 84.30 ppm in Iraq.

This study examines the mineralogical, petrographic and geochemical properties of the phosphate-containing rocks from the Upper Cretaceous Karababa Formation that outcrop in Mardin-Mazıdağı (Turkey), which is part of the Southeastern Anatolia Region. The results of these analyses will reveal the origin of the phosphate deposits in the study region. In addition to assessing the geological and mineralogical properties of the rocks, this study aims to determine the physicochemical conditions of the paleoenvironment by analyzing their major, trace and REE element composition. Comparing the detailed geochemical data that is obtained from the Arabian Plate and other similarly aged outcrops around the world is an important component in determining the marine environmental conditions prevalent during the formation of the eastern Mediterranean phosphorite belt.

1. Geological setting

The Upper Cretaceous-Paleocene Mediterranean phosphatic belt extends from southwest Turkey to Morocco and is known to be an area that is rich in phosphate. The Mazıdağı phosphate deposit is located in the northern part of the Arabian Plate in the southeastern Anatolia region (SEA) and represents the eastern Mediterranean phosphorite belt (Figure 1).

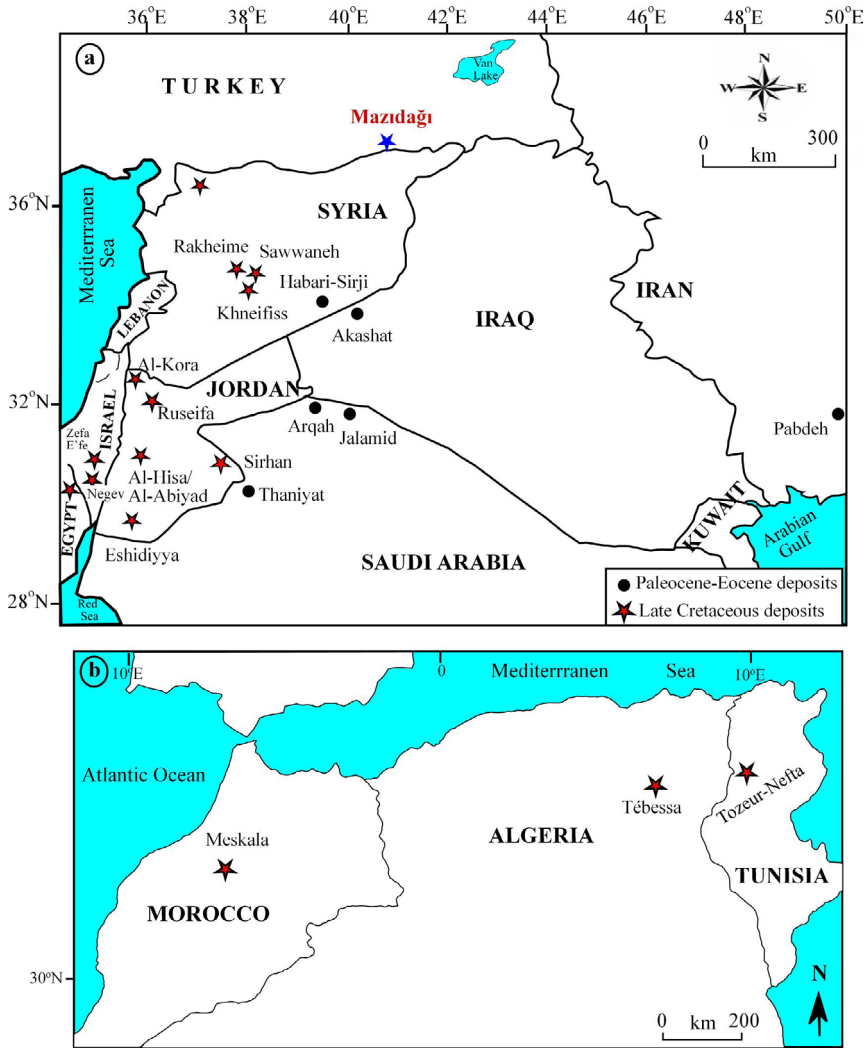

Fig. 1. Location map of the phosphorite deposits in the Mediterranean belt and adjacent countries
a) Geographical schema displaying Turkey and the Eastern Mediterranean Region;
b) Geographical schema displaying the Western Mediterranean region

Rys. 1. Mapa lokalizacji złóż fosforytów w pasie śródziemnomorskim i krajach sąsiednich
a) Schemat geograficzny przedstawiający Turcję i wschodni region Morza Śródziemnego,
b) Schemat geograficzny przedstawiający zachodni region Morza Śródziemnego

The southeastern Anatolia region includes the Bitlis-Pütürge Crystal Complex and southeast Anatolian Autochthonous (SEAA) rocks (Göncüoğlu et al. 1997). The rocks representing SEAA are located at the northern end of the Arabian Plate and consist of Precambrian-aged Cadomian base and overlying Paleozoic Tertiary-aged sedimentary rocks (Göncüoğlu et al. 1997). Phosphorite-bearing Cretaceous carbonates are located in the Mardin area (Taşıt, Kasrik, Şemikan, Akras and Mazıdağı), which constitutes the Arabian Platform (Perinçek 1980; Berker 1989; Cater and Gillcrist 1994; Okay 2008; Yilmaz et al. 2018).

The study area is located in the SEA, and stratigraphic, sedimentological and sampling studies in the field were conducted on successions representing three different members in the Mardin (Mazıdağı) region. In the northern part of the study area are the Bitlis-Zagros suture belt and the SE Anatolian ophiolite belt, and in the west, rocks belonging to the Taurus belt are found (Figure 2a). It was suggested that the Bitlis zone and its western extension, the Pütürge Metamorphites, are the deformed and metamorphosed parts of the Arabian Plate that formed during the closure of the Neotethys Sea (Göncüoğlu and Turhan 1985). The SE Anatolian Ophiolitic Belt (Yılmaz 1983), which extends along the SE Anatolian suture zone and consists of many tectonic layers, is composed of oceanic units and accretionary prism rocks that were deposited during the subduction of the southern branch of Neotethys. Considered in terms of tectonic belts (which are, from south to north, the Arabian platform, the Ekay zone, and the Nap region), and as distinguished by Yılmaz (Yılmaz 1993), the SEAA deposits are located within the Arabian platform, and the SE Anatolian Ophiolitic belt and Bitlis-Pütürge Metamorphites are located within the rocks of the Nap region (Yılmaz 1983, 2019).

In the Karababa Formation, which is the subject of this study, three different facies (inner facies with limestone and chert and the outer facies zone containing phosphate and glauconite) and two phosphate horizons were defined in the region by Beer (Beer 1966). Berker (Berker 1972) reported zones of economic ore in a large area extending between Hatay and Hakkari in the southeastern Anatolian region. According to the geochemical results of the phosphorites from the Mazıdağı-Karataş area, reserves of U_3O_8 and F reportedly existed in the region. Çoban (Çoban 1987) also identified the mineralogical compositions of phosphate formations of different structures, which consisted of Upper Cretaceous neritic limestones interbedded with Derik-Mazıdağı phosphates that were deposited during sea level rises within a shelf environment. Varol (Varol 1989) stated that the main sources of phosphorites were the zoophytoplankton (diatom)-rich organic sludge that was deposited during the Upper Cretaceous period when rising sea levels drove the Mazıdağı phosphates to bring phosphate-rich biogenic material to the shelf zone from deep water. İmamoğlu et al. (İmamoğlu et al. 2009) explained that the phosphorites of the West Kasrik member (Coniacian-Santonian) were formed by early diagenetic processes as a result of the tectonic uplift of the surrounding areas of nondetrital sediment.

Late Cretaceous-Eocene deposits belong to the Tethys Phosphorite Regime. Eastern Mediterranean (Figure 1a), north and northwest African deposits (Figure 1b), and parts of northern South America and the Caribbean (Jarvis 1992; Lucas and Prévôt-Lucas 1996;

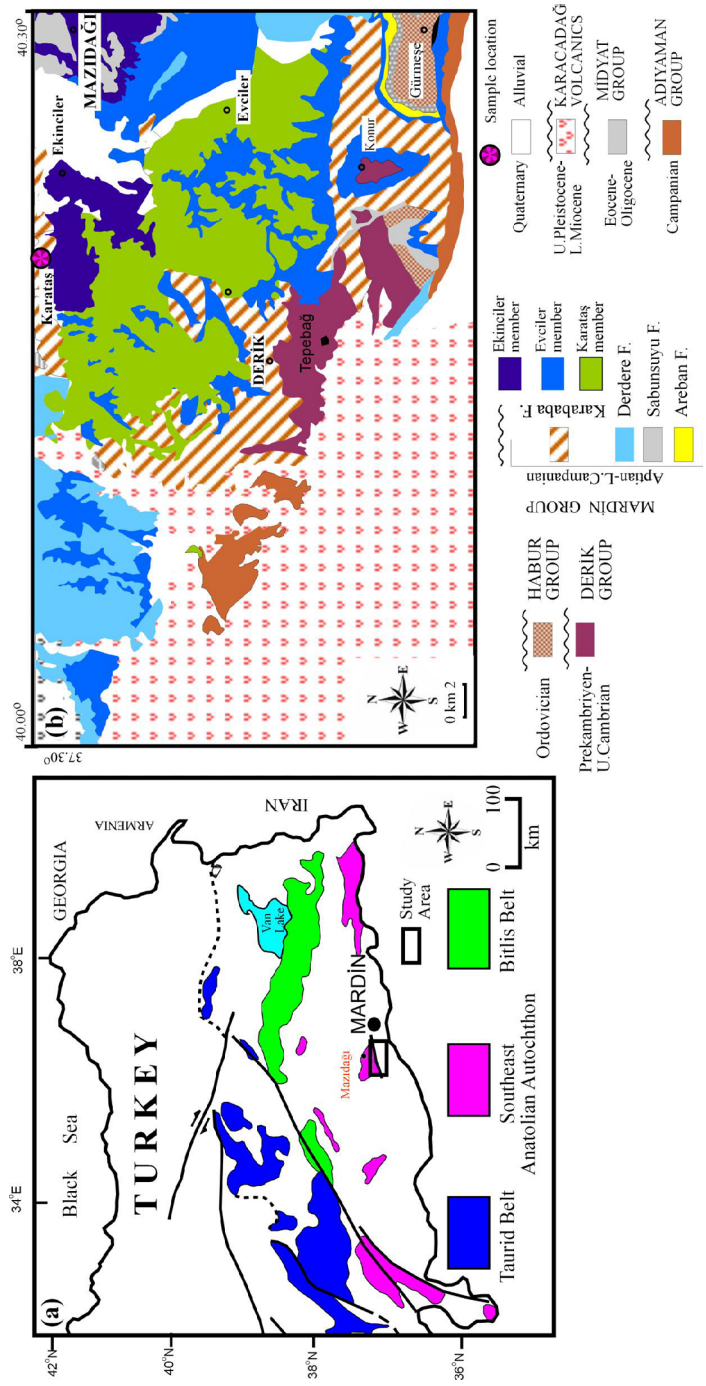

Fig. 2. a) Tectonic maps of southern Anatolia (Gönciioğlu et al. 1997);
b) Simplified geologic map of Mardin (Mazıdağı) and its vicinity (1:100,000 scaled N44 sheet) (Umut 2011)

Rys. 2. a) Mapy tektoniczne południowej Anatolii;
b) Uproszczona mapa geologiczna Mardin (Mazıdağı) i okolic (arkusz N44 w skali 1:100 000)

Follmi 1996; Soudry et al. 2006). Closure activities of the Neotethys Ocean were responsible for setting the scene for the formation of the major phosphorite deposits in the eastern Mediterranean region and throughout the Tethys belt (Soudry et al. 2006; Abed 2013; Abed et al. 2016). Major deposits were formed during Campanian to Eocene times and significantly contribute to the economic development of these countries, particularly Jordan and Syria. The phosphorite deposits of the eastern Mediterranean region (Saudi Arabia, Israel, Jordan, Iran, Iraq) are almost always associated with bedded peloids (pellets, intraclast, nodules, vertebrate fragments), chert, porcelanite, and oyster-bearing limestones, in addition to minor marl, chalk and sandstone (Powell 1989; Almogi-Labin et al. 1993; Abed 2013). The main phosphate mineral is francolite, which is a carbonate-rich variety of fluorapatite that has a relatively enhanced uranium content as a result of substitution for calcium in its crystal structure (Abed 2013). In general, Cretaceous phosphorites were formed under warm climatic conditions under shallow marine deposition conditions and at low paleolatitudes (<30°) in environments with high organic productivity and low sedimentation developed (Banerjee et al. 2020).

2. Lithology

The Upper Cretaceous-aged Karababa Formation, which is the subject of this study and belongs to the Mardin Group, was defined according to an N44 geological map at a scale of 1:100,000 (Umut 2011) and is located in the Mardin-Mazıdağı region (Karataş Village coordinates: 37°49’45’’N, 40°29’76’’E and 37°49 ‘42’’ N, 40°32’94’’E; Ekinciler Village coordinates: 37°48’15’’ N, 40°38’81’’E, and Evciler Village coordinates: 37°40’17’’N, 40°44’76’’E) (Figure 2b).

The columnar section (Figure 3a) measured in the study area showed the stratigraphic and sedimentological features of the members of the Karababa Formation within Mazıdağı (Mardin) and in its vicinity. In the southern part of the study area is the Derdere Formation (Handfield et al. 1959), which consists of Cenomanian-aged limestone and dolomites belonging to the Mardin Group. The Karababa Formation and the marine transgression, which dates between the lower Coniacian and Santonian ages (89.8 Ma), unconformably overlies the Derdere Formation. In this study, the Karababa Formation was defined and examined by dividing it into three members (Karataş, Ekinciler and Evciler) according to its phosphate content and various lithofacies properties. Typical stratigraphic and sedimentologic cross sections of the Karababa Formation were measured in three different locations, namely, the Karataş (32 m), Ekinciler (70 m), and Evciler (137 m) villages, and the total thickness was determined to be 239 m. The thirty-two-meter-thick phosphorite layers of the formation, which represented the shallow (coastal) marine environment, were named the Karataş member, and the lithological features of the succession are presented in Figure 3b.

The Karataş member begins with a five-meter-thick deposit that is gray–white in color, very fine-grained, and consists of weathered phosphorite and phosphorite with carbonate

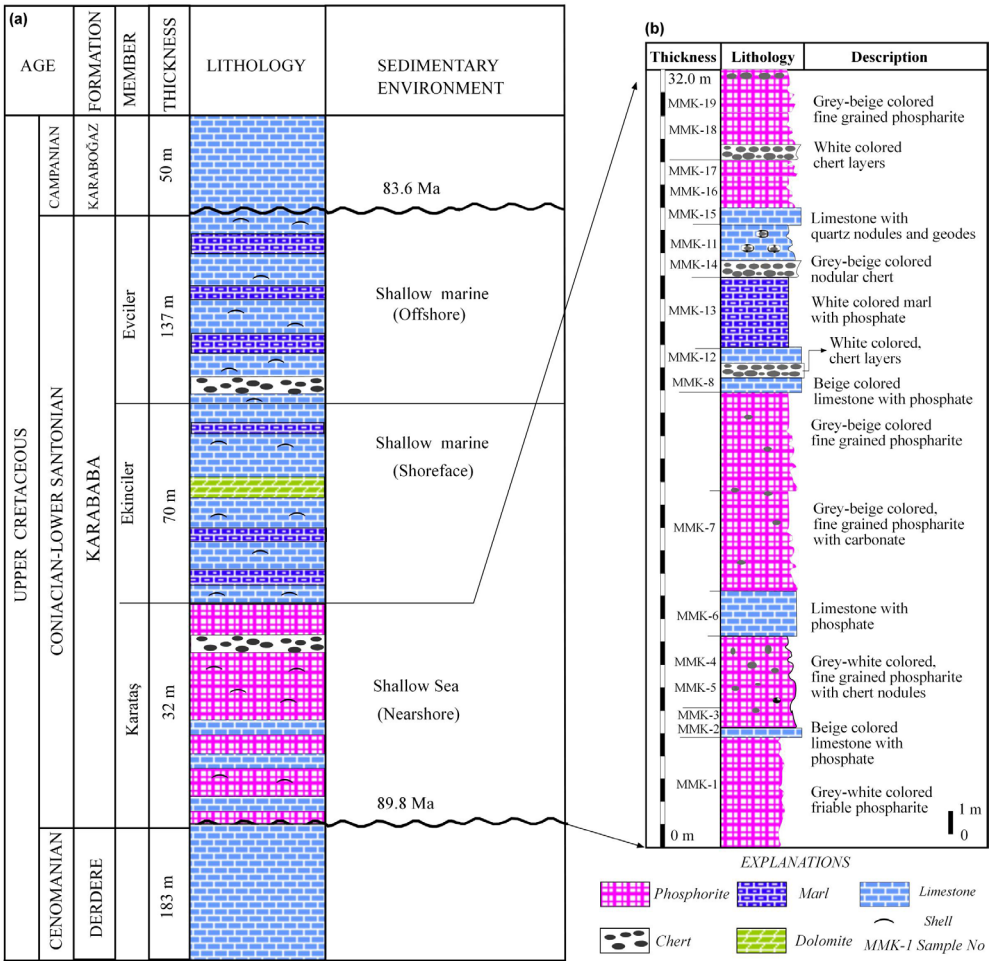

Fig. 3. a) The stratigraphic column, which is based on the measured sections, shows the interpreted sedimentary environments of the members of the Karababa Formation (Upper Cretaceous);
b) Detailed stratigraphic section of the Karababa Formation members containing phosphorite horizon

Rys. 3. a) Kolumna stratygraficzna oparta na zmierzonych przekrojach przedstawia zinterpretowane środowiska sedymentacyjne jednostek formacji Karababa (kreda górna);
b) Szczegółowy przekrój stratygraficzny jednostek formacji Karababa zawierający horyzont fosforytowy

type rocks. These layers contain very hard white ellipsoidal chert nodules that are 2–8 cm in diameter and contain abundant fossil shells (Figure 4a). The samples defined as phosphorite stand out with regard to their similarity to friable sands. Above this layer, is an approximately one-meter-thick layer of limestone that contains phosphates. Three-meter-thick layers of gray fine-grained phosphorites overlie the limestones with phosphates; these contain nodules interbedded with chert. The identified upper deposits containing phosphates consist of beige limestones and are approximately two meters thick (Figure 4b). The thicknesses of the

nodular chert layers in this area vary between 20 and 30 cm (Figure 4c). At the bottom of the limestones is a four-meter-thick bed of gray-beige phosphorites that show evidence of irregular weathering. Above this level, layers of white-beige hard carbonates with elevated phosphate contents stand out. It was observed that the beige chert nodules vary in size from 20 to 50 cm, and their internal structures exhibit geode structures consisting of concentric rings.

The Ekinciler member begins with beige limestone and has a basal thickness of ten meters (Figure 3a). The limestones are overlain by fifteen-meter-thick beige colored clayey limestones with conchoidal fractures and contain hard marl layers that are a creamy beige

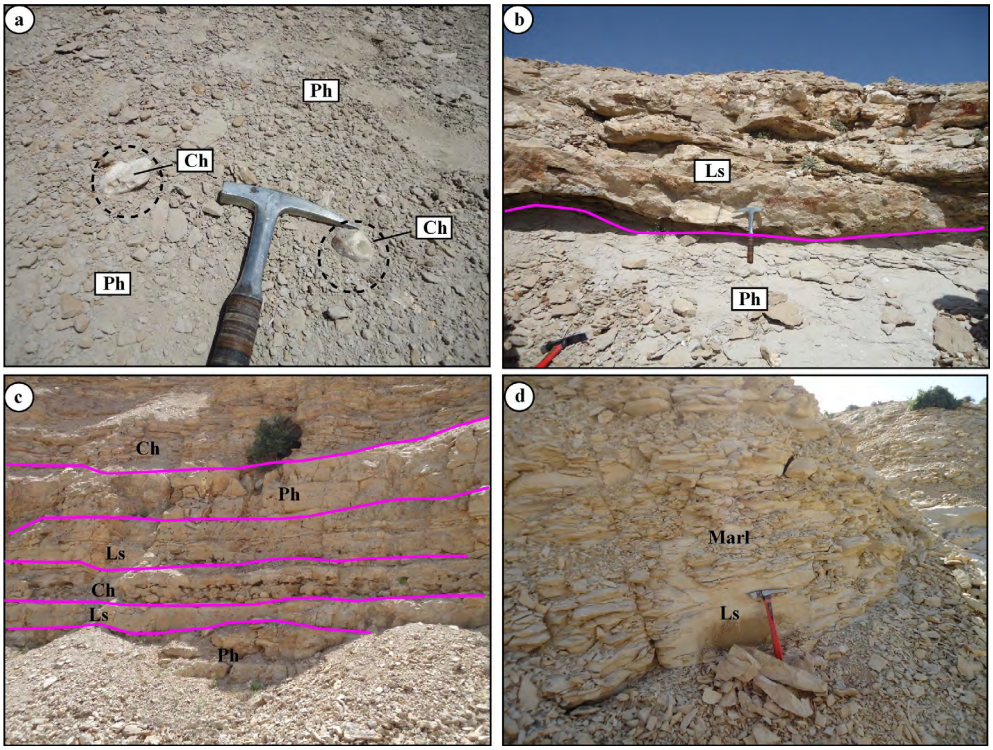

Fig. 4. Field views of the members of the Karababa Formation
a) Gray-beige colored friable phosphorite layers with white chert nodules (Karataş member); b) Gray colored friable phosphorite at the bottom and beige hard phosphatic limestone layers at the top (Karataş member); c) phosphate-bedded gray-beige colored marl layers with chert geodes and nodules (Karataş member); d) Beige colored clayey limestones with conchoidal fragments and thin hard marl layers (Ekinciler member), Ph = Phosphorite, Ls = Limestone, Ch = Chert

Rys. 4. Widoki terenowe jednostek formacji Karababa
a) Szaro-beżowe, kruche warstwy fosforytu z białymi grudkami czertu (jednostka Karataş); b) Szaro zabarwiony kruchy fosforyt na dole i beżowe warstwy twardego wapienia fosforytowego na górze (jednostka Karataş); c) Szarobeżowe warstwy margla zabarwione fosforanami z geodami i grudkami czertu (jednostka Karataş); d) Beżowe wapienie ilaste z muszlowatymi fragmentami i cienkimi warstwami twardego margla (jednostka Ekinciler), Ph = fosforyt, Ls = wapień, Ch = chert

color (Figure 4d). Dolomitic levels with cream-colored plaques were also identified at this location. In the upper parts of the dolomitic levels, a white hard clayey interbedded limestone was observed with a thickness of approximately twenty-nine meters. These layers are overlain by alternating deposits of hard beige clayey limestone and limestone interbedded with marl.

The third member, defined as the Evciler member, was deposited in the offshore environment under the active wave base, which represents the deepening part of the succession. The lithologies defined in the cross-sectional area, which has a total thickness of 137 m, are as follows: the base of the cross-section consists of an approximately ten-meter-thick hard limestone layer that contains yellowish-beige chert nodules; above the limestones is a twenty-meter-thick deposit of foliated marl layers that are gray to beige in color; these are followed by ten-meter-thick layers of cream-colored clayey limestone. It was noted that the marl layers sporadically contain chert nodules and abundant fossilized shells. It was observed that the width of the depositional environment of the Karababa Formation's transgressive succession increases toward the top.

Phosphorites occur at various stratigraphic levels of the Upper Cretaceous in Turkey, in the Karababa (Turonian–Santonian) and the Karaboğaz (Maastrichtian) formations in SE Anatolia (Berker 1989).

3. Material and methods

A total of nineteen rock samples were collected from the phosphorite levels (Karataş Member). After the samples were washed, they were sliced into thin sections, and crushed, pulverized, and sieved before being subjected to clay separation, X-ray diffraction (XRD), and optical microscopy (OM). These processes and analyses were conducted within the Mineralogy and Petrography Research Laboratories of the Geological Engineering Department of Batman University. A trinocular polarized microscope (LEICA DM 750P) and a scanning electron microscope (SEM) were used for petrographic examinations. Secondary electron scanning electron microscopy (SEM-SE) and backscattered electron microscopy (SEM-BSE) imaging processes and energy dispersive spectrometry (EDS) analyses were performed in the Laboratories of MTA (General Directorate of Mineral Research and Exploration, Turkey). The SEM examinations were made with a SEM JEOL JSM-6490 LV model scanning electron microscope that included the IXRF-EDS system. The instrumental conditions were set as time constant (TC) = 32.0, kV = 20.0, and WD = 22 mm.

In this study, the X-ray diffraction (XRD) method was used to determine the mineralogical compositions of the samples, and the analyses were performed using the diffractograms obtained in a Rigaku MiniFlex-II model device (CuKα = 1.541871 Å). Whole-rock and clay-size components (<2 μm) were identified in the samples taken from the formation (JCPDS 1990), and their semiquantitative percentages were identified based on the external standard

method (Brindley 1980). Clay fractions (grain sizes of <2 μm) were separated by dispersing the bulk sample in distilled water after acid treatment to eliminate carbonate minerals (5% acetic acid or 5% hydrochloric acid for calcite and dolomite minerals, pH = 6.0–7.0; Brown 1961; Caillere and Henin 1963; Brindley and Brown 1980). This was followed by sedimentation and centrifugation. Oriented clay fractions were obtained by thin-smears of clay paste on glass slides. XRD patterns were obtained for air-dried, ethylene-glycolated samples that were heated to 490°C for four hours (Brown 1961; Caillere and Henin 1963; Brindley and Brown 1980). The clay mineralogy was determined from the XRD results following Moore and Reynolds (Moore and Reynolds 1997).

Selected samples of phosphorites (n = 11) from the Karataş Member were measured for trace and rare earth elements. The major and trace element analyses in the phosphorites were performed by Acme Laboratories LLC in Canada (Acmelabs). The apatite samples were fused with lithium metaborate/tetraborate, and the resulting bead was dissolved in a weak solution of nitric acid. This is the only method of dissolving major oxides, including SiO_2, refractory minerals (i.e., zircon, sphene, monazite, chromite, gahnite, etc.), REEs and other high field strength elements. Analytical code LF-200 was used for the geochemical analysis of phosphorite samples, and the standard reference material STD-SO-19 was used for calibration. ICP-OES methods were followed during the major element analyses, while ICP-MS methods were used for the trace/rare and rare earth element (REE) analyses. The details of the analysis methods and instrumental detection limits are available on the company's website (Acmelab 2023).

4. Petrography and mineralogy

The phosphate-rich rocks observed in the areas that represent the Karataş member of the Karababa Formation have a micritic matrix, and the allochems mostly consisted of bioclasts (pellet, bone and rock fragments) (Figure 5a). The textural features of these rocks were labeled according to Folk (1962), who considered their allochemical, orthochemical, and mineralogical compositions. In particular, based on the abundance of apatite minerals (>15%) (determined by XRD), which represent the phosphatized composition of pellets and bone fragments, the prefix "phospho-" was used when naming certain rocks. The rock name "phosphorite" is taken here to mean a sedimentary rock in which 50% or more of its volume is composed of phosphate components (specifically, carbonate fluorapatite) (Al-Bassam et al. 2010). The pellets have sizes varying between 50 and 200 μm. While some apatitic pellet types transmit light, some types do not transmit polarized light and have an isotropic appearance (pseudoapatite) (Figure 5b). Bone fragments are observed in colorless platy and prismatic shapes (Figure 5c). Isotropic-appearing pellets and differently shaped bones and tooth remnants were common in these rocks. Quartz-filled fossils, which are thought to be bone fragments, ranging in size between 500 and 2000 μm, were also identified (Figure 5d).

SEM analyses of the samples classified as phosphorite showed that the apatite minerals had spherical and ellipsoidal shapes, and their sizes ranged between 100 and 200 µm (Figure 6a). The P, Ca, and F content of the apatite minerals were identified via EDS (Figure 6b). The EDS analyses of apatite revealed P_2O_5 (38.11 wt.%), CaO (52.46 wt.%), F (7.18 wt.%), and Na_2O (2.58 wt.%). The chemical composition obtained from these results was compatible with the carbonate fluorapatite (CFA) identification, as determined by XRD. The intergranular space was filled with cement material (carbonate, microcrystalline apatite, clay minerals). The independent appearance of apatite minerals in cement composed

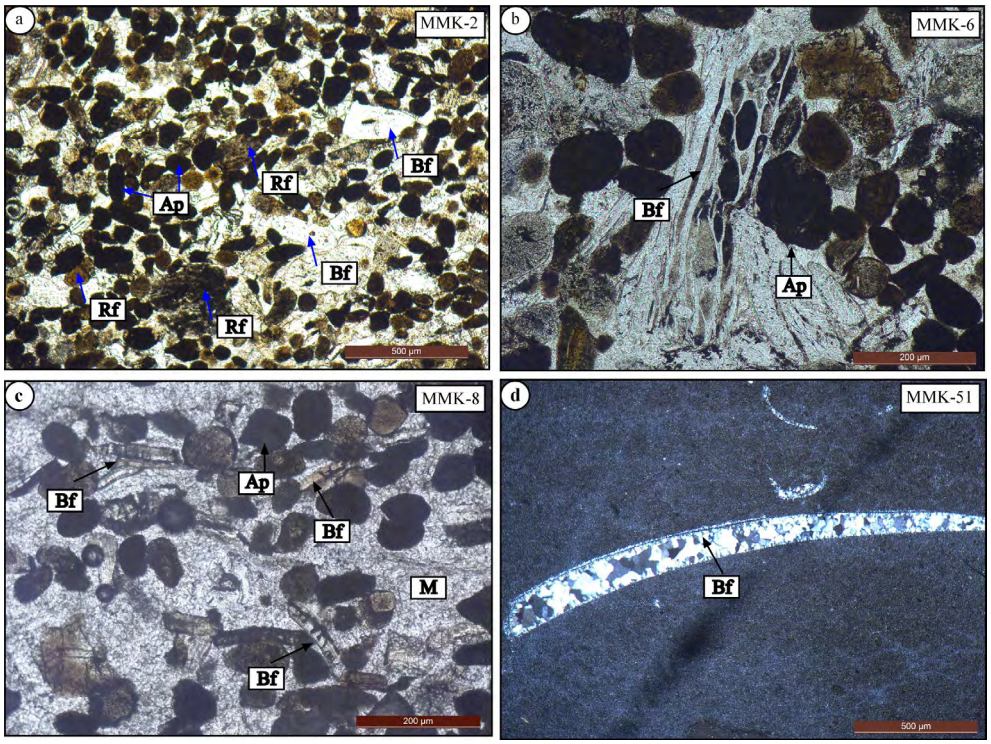

Fig. 5. Optical microscopic photographs show phosphorites of the Karababa Formation (Karataş member) a) Isotropic pelletic apatite minerals, plate bone fragments and rock fragments in the phosphomicrite matrix (crossed polarized light = CPL); b) Optical isotropic pelletic apatite minerals and platy bone fragments developed in limestones in the phosphomicrite matrix (CPL); c) Isotropic-looking pelletic apatite minerals and phosphatized large angular and prismatic bone fragments (plane polarized light = PPL) in the phosphorite rocks; d) Silica-filled subangular bone fragment in the chert sample (CPL)
Ap – Apatite, Bf – Bone fragments, Rf – Rock fragments

Rys. 5. Zdjęcia z mikroskopu optycznego przedstawiają fosforyty formacji Karababa (jednostka Karataş); a) Izotropowe granulowane minerały apatytowe, fragmenty płytek kostnych i fragmenty skał w matrycy fosfomikrytowej (światło spolaryzowane skrzyżowanie = CPL); b) Optycznie izotropowe granulowane minerały apatytowe i fragmenty płytek kości powstałe w wapieniach matrycy fosfomikrytowej (CPL); c) Izotropowo wyglądające granulowane minerały apatytowe i fosforanowane duże kanciaste i pryzmatyczne fragmenty kości (światło spolaryzowane w płaszczyźnie = PPL) w skałach fosforytowych; d) Nieco kanciasty fragment kości wypełniony krzemionką w próbce czertu (CPL); Ap – apatyt, Bf – fragmenty kości, Rf – fragmenty skał

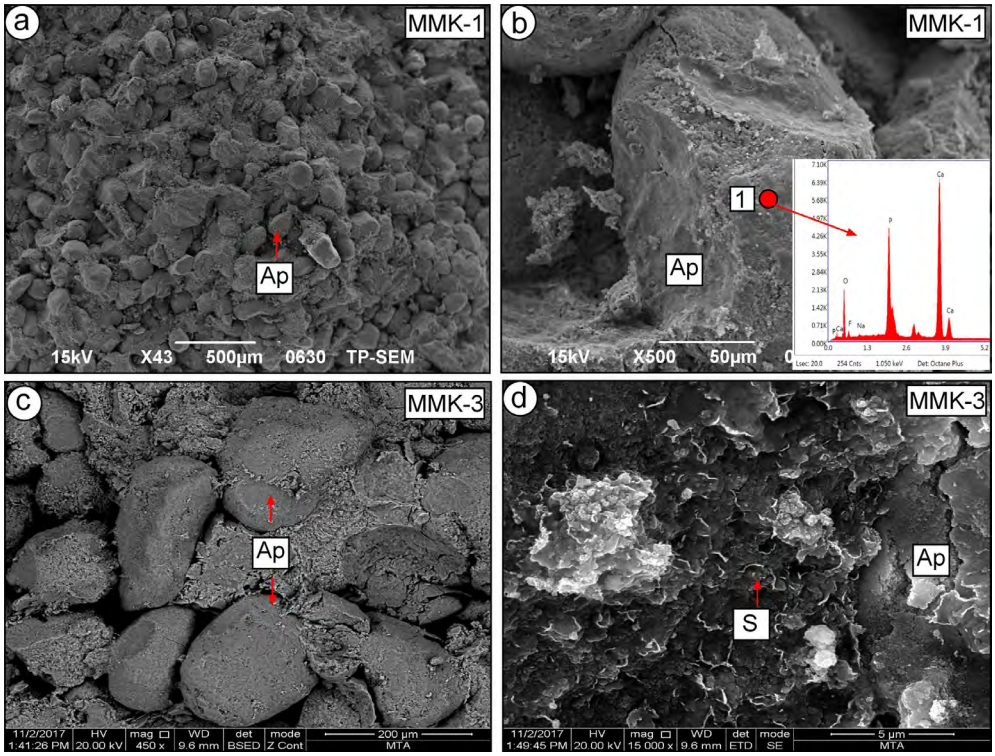

Fig. 6. SEM microphotographs of the Karababa Formation members phosphorite rocks
a) Ellipsoidal phosphatic peloids and bone fragments in microcrystalline calcareous/apatitic cement; b) Ellipsoidal apatitic peloids and elemental spectrum results (1 = EDS spectrum point); c) Microcrystalline carbonate and apatitic cement enclosure large-grained apatite minerals; d) Smectite minerals formed in pores of phosphorite rock; Ap = Apatite, S = Smectite

Rys. 6. Mikrofotografie SEM skał fosforytowych jednostek formacji Karababa
a) Elipsoidalne peloidy fosforanowe i fragmenty kości w mikrokrystalicznym cemencie wapiennym/apatytowym; b) Elipsoidalne peloidy apatytowe i wyniki widma elementarnego (1 = punkt widma EDS); c) Węglany mikrokrystaliczne i cement apatytowy otoczone gruboziarnistymi minerałami apatytowymi; d) Minerały smektytu powstałe w porach skały fosforytowej
Ap = apatyt, S = smektyt

of calcite and/or microcrystalline apatite suggested that these minerals were formed from biogenic sources (e.g. bone, fossil fragment, and shell) (Figure 6c, d).

Apatite minerals were found with a thick plate-like appearance in some rocks. These formations were probably considered to be phosphated bone fragments. In the biomicrosparite sample, there were different types of fossil shells in microsparitic cement (Figure 7a). Leafy smectite formations were detected in the pores of these samples and the matrix. Phosphated fish bone fragments were observed within elongated and plate-like shapes (Figure 7b). Palygorskite formations, in the form of fibrous balls, were observed in the matrix of the marl samples collected from the formation. The palygorskite samples were composed of

fibers longer than 2 μm (Figure 7c). Palygorskite/sepiolite fibers, which were occasionally arranged in a long and thin radial or lattice appearance, were estimated to be larger than 8 μm. Another type of clay mineral involved in paragenesis in the marl samples is represented by mixed layers of chlorite-vermiculite (C-V), and this mineral was deposited in thick foliations (Figure 7d).

Quantitative X-ray diffraction (XRD) analysis was used to determine the complete mineralogy of the rock and clay fraction of the Karataş member (Table 1). Apatite, calcite,

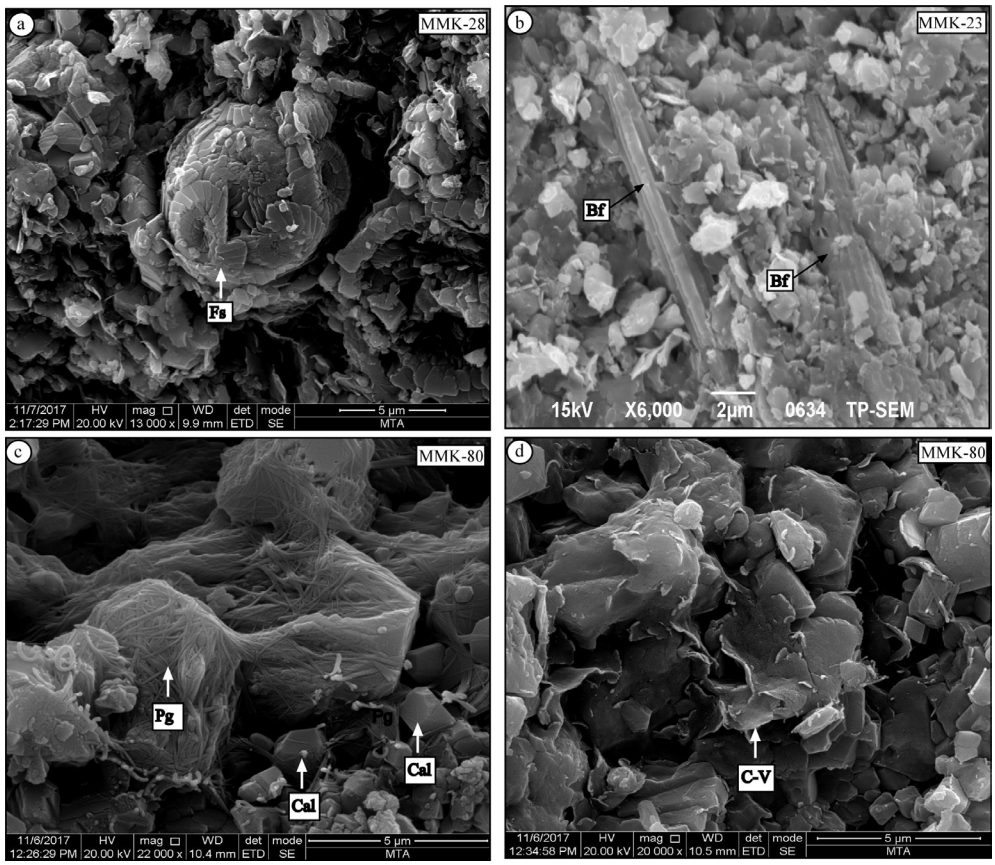

Fig. 7. SEM microphotographs of rocks relating to the Karababa Formation (Ekinciler and Evciler members) a) Calcareous nannoplankton shell in the biomicrosparite samples; b) Biomicrosparite sample with platy bone fragments and leafy clay minerals; c) Fibrous palygorskite tangles in the matrix and euhedral calcite minerals in marl; d) Mixed-layered clay minerals (C-V) with thick leaf shapes
MMK-28 = sample no, Fs = Fossil, Bf = Bone fragment, Pg = Palygorskite, C-V = Chlorite-Vermiculite

Rys. 7. Mikrofotografie SEM skał związanych z formacją Karababa (jednostki Ekinciler i Evciler)
a) Wapienna skorupa nannoplanktonu w próbkach biomikrosparytu; b) Próbka biomikrosparytu z blaszkowatymi fragmentami kości i liśćmi minerałów ilastych; c) Włókniste sploty palygorskitu w matrycy i euhedralne minerały kalcytu w marglu; d) Mieszane warstwowe minerały ilaste (C-V) o grubych kształtach liści
MMK-28 = nr próbki, Fs = skamielina, Bf = fragment kości, Pg = palygorskit, C-V = chloryt-wermikulit

Table 1. Semi-quantitative X-ray diffraction (XRD) analysis results showing the whole-rock and clay fraction mineralogy of the Karataş phosphorite member in the Mardin-Mazıdağı area

Tabela 1. Wyniki półilościowej analizy dyfrakcji rentgenowskiej (XRD) przedstawiające mineralogię frakcji całej skały i gliny jednostki fosforytowej Karataş w obszarze Mardin-Mazıdağı

Sample No	Whole Rock						Clay Fraction						Rock name (Folk 1962; Al-Bassam et al. 2010)
	Cal	Dol	Qz	Ps	Ap	O-CT	S	Pg/Sp	I	K	I-V	C-V	
MMK -1					100								Phosphorite
MMK -2	55				45								Limestone with phosphate
MMK -3					100								Phosphorite
MMK -4					100								Phosphorite
MMK -5			100										Chert
MMK -6	70				30								Limestone with phosphate
MMK -7	35		3		62								Phosphorite with carbonate
MMK -8	65		3		32								Limestone with phosphate
MMK -9	100												Limestone
MMK -11	86		14										Limestone with siliceous
MMK -12			100										Chert
MMK -13	46		28	12	14			35	30			35	Marl with phosphate
MMK -14			100										Chert
MMK -15	100												Limestone
MMK -16			2		98								Phosphorite
MMK -17			15	10	50	25			38	29	33		Phosphorite
MMK -18			4		96								Phosphorite
MMK -19			25	10	50	15	30	17	35	18			Phosphorite with siliceous

Cal = Calcite, Dol = Dolomite, Qz = Quartz, Ps = Phyllosilicate, Ap = Apatite, O-CT = Opal-CT, S = Smectite, Pg/Sp = Palygorskite/Sepiolite, I = Illite, K = Kaolinite, I-V = Illite-vermiculite, C-V = Chlorite-vermiculite.

quartz, a lower amount of opal-CT (microcrystalline cristobalite) and phyllosilicate (illite, smectite, palygorskite/sepiolite, kaolinite, the mixed layered C-V and I-V) minerals were present in the phosphorite (i.e. phosphorite without carbonate, phosphorite with carbonate) and other rocks (i.e. Phosphate- and silica-bearing limestone and marl). In the phosphorite rocks, apatite minerals were identified by peaks at 2.78 Å, which correspond to the (211)

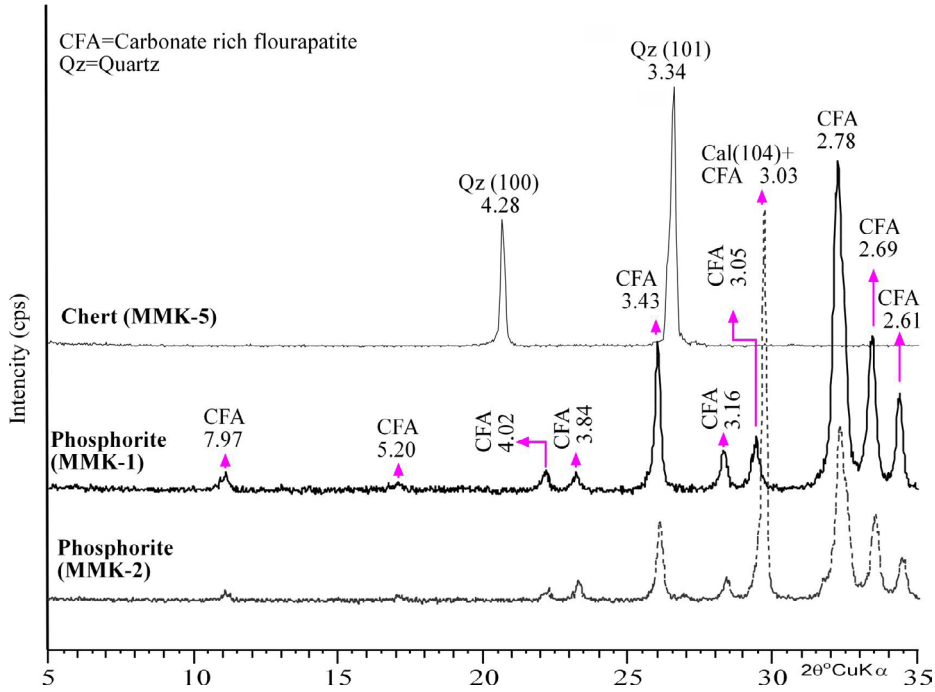

Fig. 8. XRD whole-rock diffractograms of phosphorites (Karataş member) (sample no: MMK-1 and MMK-2) and chert (sample no: MMK-5)

Rys. 8. Dyfraktogramy XRD całej skały fosforytów (jednostka Karataş) (próbka nr: MMK-1 i MMK-2) i czert (próbka nr: MMK-5)

surface, and 3.43 Å, which corresponds to the (002) surface (Figure 8). The most common form of apatite paragenesis was observed to be occasionally accompanied by calcite and quartz. The rocks defined as phosphated limestone were represented by apatite (<50%) and accompanied by higher amounts of calcite (>50%) minerals. The peaks observed at 3.03 Å, corresponding to the surface of calcite (104), were distinguished due their higher intensity in comparison to those of apatite when the pure apatite composition was examined (Figure 8). The marl of the Evciler member mainly contain palygorskite/sepiolite, some illite, chlorite, and mixed layers of C-V clay minerals (Figure 9a, b).

5. Chemical composition of phosphorites

To compare the major and rare earth element compositions of average Mazıdağı phosphorites (n = 11) analyzed ICP-MS method, the average world phosphorite (AWP: Altschuler 1980) and seawater (SW: Høgdahl et al. 1968) elemental compositions were used. The details are given in Table 2.

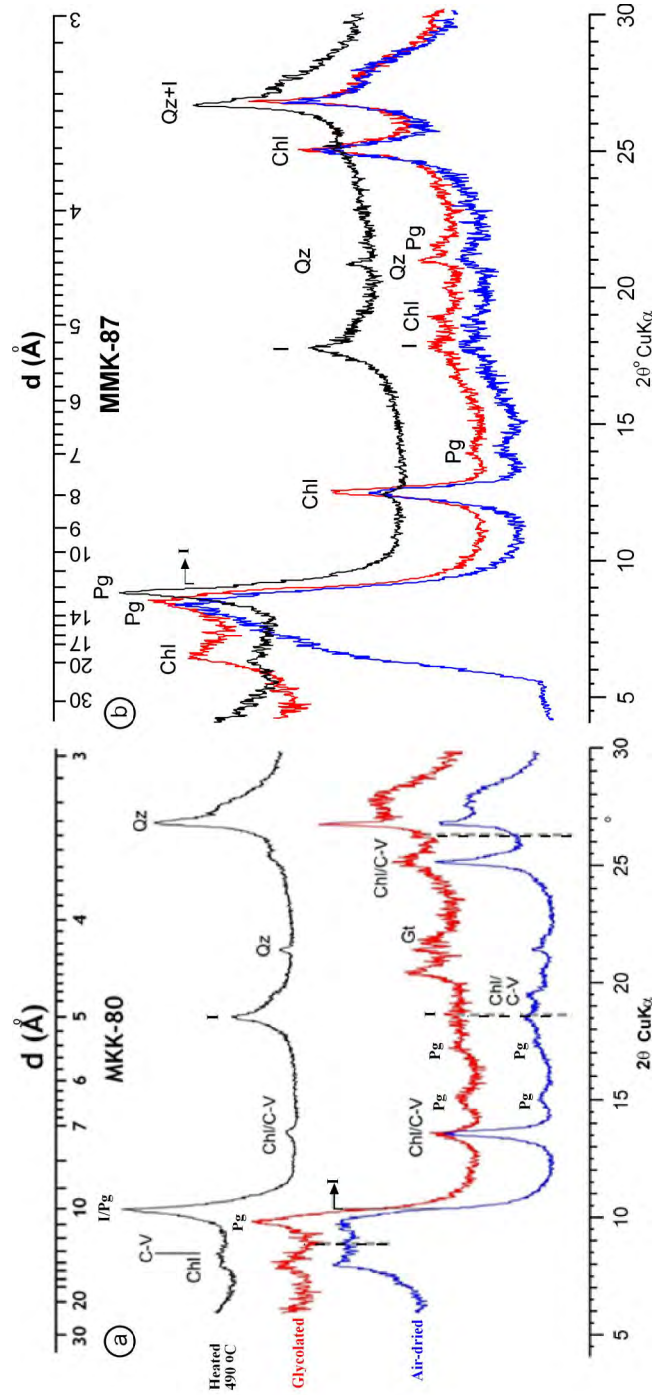

Fig. 9. XRD patterns of oriented clay fractions of the Karababa Formation

a) Sample no: MMK-80; b) Sample no: MMK-87; Chl = Chlorite, Gt = Goethite, Pg = Palygorskite, Qz = Quartz, I = Illite, C-V = Chlorite-vermiculite

Rys. 9. Dyfraktogramy XRD orientowanych frakcji ilastych formacji Karababa

a) Numer próbki: MMK-80; b) Próbka nr: MMK-87; Chl = chloryt, Gt = goetyt, Pg = palygorskit, Qz = kwarc, I = illit, C-V = chloryt-wermikulit

Table 2. Major oxide (wt.%) and some trace element concentrations (ppm) of the representative apatite samples were analyzed by ICP-OES and ICP-MS from the Mazıdağı phosphorites (average), and geochemical data were analyzed from the AWP (Average World Phosphorite) and SW (seawater) compositions

Tabela 2. Stężenia głównych tlenków (% wag.) i niektórych pierwiastków śladowych (ppm) reprezentatywnych próbek apatytu analizowano za pomocą ICP-OES i ICP-MS z fosforytów Mazıdağı (średnia), a dane geochemiczne analizowano z AWP (Average World Phosphorite) i SW (woda morska)

Oxide (%)/ /Sample no	Mazıdağı phosphorites (average, n = 11)	Rare Earth element (ppm)	Mazıdağı phosphorites (average, n = 11)	AWP[1]	SW[2]
P_2O_5	35.41	La	16.25	133	3.40
SiO_2	0.79	Ce	5.15	104	1.20
TiO_2	0.02	Pr	1.84	21	0.60
Al_2O_3	0.16	Nd	7.90	98	2.8
Fe_2O_3	0.08	Sm	1.39	20	0.45
MnO	0.01	Eu	0.37	6.5	0.13
MgO	0.19	Gd	2.41	12.8	0.70
CaO	54.88	Tb	0.38		0.14
Na_2O	0.75	Dy	2.66	19.2	0.91
K_2O	0.03	Ho	0.75	4.2	0.22
LOI	7.39	Er	2.47	23.3	0.87
		Tm	0.35		0.17
		Yb	2.31	12.6	0.82
		Lu	0.40	2.7	0.15
		∑REE	44.57	457.30	12.56
		Y/Ho	70.47		
		Ce_{anom}*	–0.30	1.63	–0.98
		Ce/Ce^*_{NASC}	0.18	0.40	0.17
		Ce/La	0.32	0.78	0.35
		V/(V+Ni)	0.93		
		V/Ni	14.85		

[1] Høgdahl et al. 1968; [2] Altschuler 1980.

Average oxide concentrations in phosphorites are 54.88 wt.% CaO and 35.41 wt.% P_2O_5 with SiO_2, Fe_2O_3, Al_2O_3, Na_2O, MgO, and K_2O being less than 1 wt.%. High P_2O_5 and CaO values in carbonate fluorapatite, ion composition and pH values of sea water are useful indicators due to diagenetic phosphatization during high oxidizing conditions of the basin (Ames 1959; Krumbein and Garrels 1952; Nathan and Sass 1981; Abou El-Anwar et al. 2016).

Trace element of the Mazıdağı phosphorites and other deposits of Arabian countries (Israel: Panczer et al. 1989) were normalized according to the North American Shale Composite (NASC) values (Figure 10). NASC values were taken from Condie (Condie 1993) for Nb and Y and from Gromet et al. (Gromet et al. 1984) for other elements. The total trace element concentrations normalized to NASC values (ppm) of the phosphorites were 10.65 for Sr, 1430.81 for P, 20.90 ppm for U, and 1.51 ppm for Y. The apatite minerals show positive anomalies for Ba, U, Ta, La, Sr, P, Sm, and Y, but had negative anomalies for Th, K, Nb, Ce, Nd, Hf, and Ti. There is a positive Eu anomaly in phosphorites. Positive Eu anomalies have also been widely reported in reducing conditions and high-temperature modern deep-sea hydrothermal systems (Douville et al. 1999; Michard et al. 1983; Owen and Olivarez 1988; Khan et al. 2012a, 2012b; Kechiched et al. 2020). Compared to the other Middle Eastern–North African phosphorites such as those from Saudi Arabia, Iran, Iraq, Israel and Morocco, phosphorites such as those from Jordan, the Upper Cretaceous phosphorites in Turkey, have higher contents of P (1430.81 ppm) (Figure 10). A positive trend is marked by high contents of Sr, and low contents of K and Ti, reflecting early diagenetic phase with the rate of organic matter indicated by the mean contents of Mn and Cu. In addition, the phosphates of the Mazıdağı phosphorites recorded some trace and rare earth elements such as V, Nb and Hf, which are not detected in the other Arabian countries, which can be related to the high content of organic matter.

Values of rare earth element (REE) for phosphorites were compared for Saudi Arabia (Al-Hobaib et al. 2013), Iraq (Aba-Hussain et al. 2010), Jordan (Abed et al. 2016), Morocco

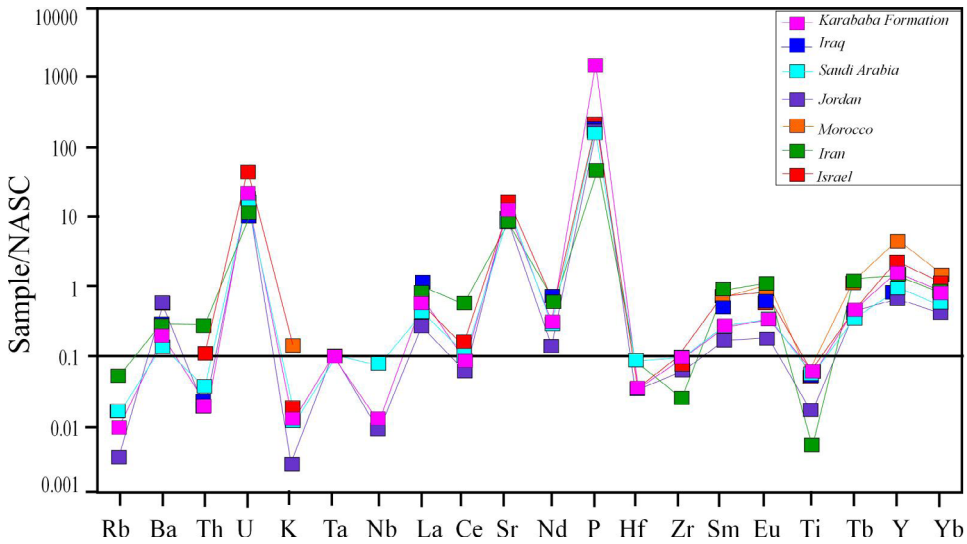

Fig. 10. NASC-normalized trace element patterns of the composition of the Mazıdağı phosphorites (average value, n = 11), Arabian plate and nearby deposits (Gromet et al. 1984)

Rys. 10. Znormalizowane wzorce pierwiastków śladowych NASC składu fosforytów Mazıdağı (średnia wartość, n = 11), płyta arabska i pobliskich złoża

(Amine et al. 2019) and Iran (Zarasvandi et al. 2021), seawater (SW; Høgdahl et al. 1968) and average world phosphorites (AWP; Altschuler 1980) (Figure 11). An enrichment of factor 1 to 31 was observed for the La-Lu concentration in the phosphorites. According to the NASC values, the patterns of the phosphorites, Iraq, AWP and SW trace element compositions differed from each other and indicated enrichment and depletion. The NASC-normalized REE patterns of the phosphorites were higher than the SW composition and much lower than the AWP, and the total REE concentration levels were between 44.44 and 44.69 ppm (average: 44.57 ppm). The concentrations of the light rare earth elements (LREE = La, Ce, Pr, Nd, Pm, Sm, Eu, Gd) within the apatite minerals showed a decrease compared to the heavy rare earth elements (HREE = Tb, Dy, Ho, Er, Tm, Yb, Lu, Y). The REE content of the AWP (Altschuler 1980) is 457.30 ppm, while SW contains only 12.56 ppm. Low REE values in phosphate formations are due to biogenic components in the phosphogenic system, physicochemical conditions, contact time with seawater and postdepositional changes (McArthur and Walsh 1984; Wright et al. 1987; Shields and Stille 2001). The REE distributions indicative of sea-level rises fit the HREE-enriched seawater model and show a negative Ce anomaly (Shields and Stille 2001). The low REE values observed in the Mazıdağı phosphorites may be related to the fact that the physicochemical and postdepositional conditions in the basin did not change after deposition and the detrital return was low. The REE distribution patterns of the studied rocks is similar to global seawater (Figure 11). ΣREE of Mazıdağı phosphorites samples of Mardin are very lower (n = 11; 44.57 ppm) compared to the marine phosphorite average (~700 ppm; Altschuler 1980). Compared to other equivalent phosphorites in the Arabian Plate, Mazıdağı REEs patterns are very similar to Saudi Arabian phosphorites. The REEs distribution patterns of the Mazıdağı phosphorite samples from Mardin are very similar and are also comparable with REEs patterns from other

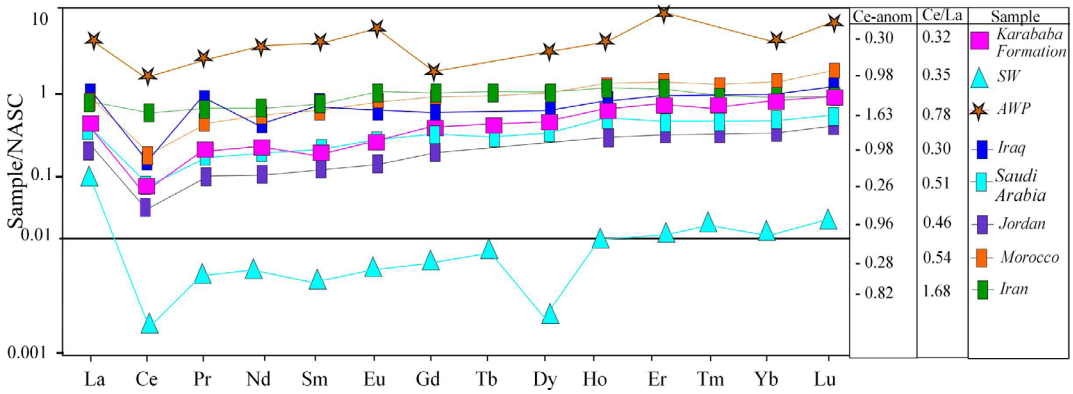

Fig. 11. NASC-normalized REE patterns of the Mazıdağı phosphorites (average value, n = 11), seawater (SW: Høgdahl et al. 1968), AWP (Altschuler 1980), Arabian plate countries and other composition

Rys. 11. Znormalizowane wzorce REE NASC fosforytów Mazıdağı (średnia wartość, n = 11), woda morska (SW: Høgdahl i in. 1968), AWP (Altschuler 1980), kraje płyty arabskiej i inny skład

phosphorites in Arabian and African plates. The enrichment of REEs in francolite, where REE substitutes for Ca in the francolite lattice (Jarvis et al. 1994; Piper 1999), has been recognized for more than a century (Jarvis et al. 1994). Deviations in REEs abundance in phosphate phases have primarily been interpreted as a direct result of secular changes in the chemistry of the ocean (Wright et al. 1987; Picard et al. 2002; Lécuyer et al. 2004).

In phosphatization, redox conditions are evaluated based on many parameters. One of these is the Ce anomaly, which was calculated by normalizing values according to the NASC protocol used in this study

$(Ce_{anom} = [Log\ (3 \times Ce_{sample}/Ce_{NASC})\ (2 \times La_{samp}/La_{NASC}) + (Nd_{samp}/Nd_{NASC})]$ (Wright et al. 1987). The Ce anomaly was low for the phosphorites with negative values such as –0.28 and –0.32.

6. Discussion

During the Cretaceous-Tertiary (CT) transition (65 Ma ago) biogenic changes driven by changing sea levels caused an increase in phosphorus concentration in the marine photic zone (Cook P.J. and Cook J.R. 1985). This transition resulted in the extinction of many species (Alvarez et al. 1980). Therefore, during the Cretaceous-Tertiary (CT) transition, thick layers of phosphorus were deposited due to marine biogeochemical processes driven by mass extinctions in many parts of the world. Shell, bone, and skeletal fragments were phosphatized in slightly oxic conditions before being reworked in the shallow and more oxygenated marine environment formed by the Cretaceous marine transgression.

It has been stated that the distribution of phosphate deposits on earth depends on the phosphogenesis periods and that some of the reasons for these phosphogenesis peaks are the latitude-longitude changes within marine environments and compositional changes in the oceans (Cook and McElhinny 1979; Arthur and Jenkyns 1981). It has also been reported that the origin of the Upper Cretaceous economic phosphate deposits that have been associated with the evolution of the Southern Tethys Ocean is closely related to the samples found in Africa and the Middle East (Lucas and Prévôt-Lucas 1996; Bardet et al. 2000). Regional comparisons between the Middle East and southeastern Turkey indicate that the marine transgression that deposited the phosphorite formations are of a regional nature. This study considered that the mineral formation processes were dependent on the biogenic and biogeochemical activities that occurred in conjunction with changes in the level driven by tectonic shifts in the basin during the CT period.

The data obtained from the mineralogical and geochemical analyses performed on the Upper Cretaceous (lower Aptian to Campanian) Karababa Formation in the Mardin-Mazıdağı region during this study are discussed in this section. According to the XRD-WR results, the phosphorites in the Karataş member included $Ca_5(PO_4)_3F$ (carbonate fluorapatite; CFA) in their composition. Marine phosphate minerals are mostly reported in CFA formations. Depending on the biogeochemical activity in the seas, organically-derived phosphorus (P)

begins to condense in seawater. In general, apatite minerals are formed authigenically during diagenetic processes in marine environments with high sediment loads that are supersaturated with respect to phosphorus. Low detrital return at the phosphate-containing layers and the loose lithological texture of the phosphorite formations indicate rapid tectonic uplift in the basin. Therefore, the presence of a small amount of cement material (carbonate, clay) in petrographic studies reveals that rapid sedimentation occurred within a low-energy or shallow marine (i.e., coastal) environment. The diagenesis stage does not fully occur at these levels (in terms of the degree of cementation) in these types of environments. Ce/Ce* – Nd ratios in geochemical data support this view.

Sepiolite/palygorskite minerals in Tertiary rocks occur widely as diagenetic, pedogenic, and newly formed minerals and were formed in different sedimentary environments (e.g., lake, lagoon, and sea) (Singer 1979; Singer and Galan 1984). In marine environments, phosphate-related palygorskite minerals were first studied in the Eocene deposits of the West African coastal basins (Slansky et al. 1959), and it is widely accepted that these clays were formed by authigenic processes in the deep oceanic environment (Bowles et al. 1971; Couture 1977; Church and Velde 1979; Tlili et al. 2010; Nathan and Soudry 2018). The observation of sepiolite/palygorskite and smectite minerals in the pores and the matrix by SEM has supported interpretations regarding their authigenic precipitation (Millot 1970; Singer 1979; Weaver 1984; Isphording 1984; Estéoule-Choux 1984; Singer 1984; Chahi et al. 1993; Torres-Ruiz et al. 1994; Yalçın and Bozkaya 1995).

The formation of mixed-layered clays involved solid-state transformation and dissolution/crystallization mechanisms (Srodon 1999). The mixed layered clay beds commonly observed during diagenesis are C-S, C-V, and I-S. C-V beds are a step in the aggregation sequence within which the 2:1 bedded vermiculite evolves into chlorite (Dunoyer de Segonzac 1970; Hoffman and Hower 1979). Therefore, formations with mixed-layered clays, such as C-V and I-V, observed in the formation were believed to have formed as a result of dissolution, redeposition, and neoformation/transformation from other minerals (e.g., muscovite, biotite, chlorite).

According to the results of the geochemical analyses, phosphorites in the Karababa Formation have high amounts of P_2O_5 (average 35.41 wt.%), which represents high-grade phosphate. The mean P_2O_5 levels of the Upper Cretaceous and Paleocene phosphate-containing deposits on the Arabian plate are as follows: 25.67 wt.% for Egypt (Duwi Formation) (Abou El-Anwar et al. 2017), 23.0 wt.% for Saudi Arabia (Sirhan-Turaif basin) (Meissner and Ankary 1970), and 22.0 wt.% for Iraq (Akashat) (Benni 2013). In terms of mean values, the value determined in this study was 35.41 wt.%, which indicates higher rates of P_2O_5 as compared to similarly aged deposits. This result was probably because the region is located in a shallow area where the depth of water in the basin gradually decreased. As a result, there was improvement in the biogeochemical conditions of the environments occupied by the skeletal and shell-derived organisms (mollusks, fish, etc.) that would eventually form the main rocks required for phosphorite formation. These conditions seem to have provided the diagenetic origin of the phosphorite formations which began from the biological residues in the basin, where solar energy is abundant in an oxygen-rich environment.

A low Fe_2O_3 value (in this study, average: 0.08 wt.%) in the phosphorites was interpreted as relating to the development of phosphorite formations within a slightly oxidized environment (Choquette and James 1990). Furthermore, low Ce_{anom} values in apatites confirm these views. It is known that trace element distributions vary depending on the oxidation zone and that high concentrations of Sr, As, and La are related to the oxidation and erosion of organic matter. Mazıdağı phosphorites were determined to identify oxic conditions with a low Ce anomaly mean of –0.30 (0.28–0.32), low Ce/La ratios of 0.32 (0.28–0.35), and a V/(V + Ni) mean of 0.93 (0.91–0.95). The low REE content and negative Ce_{anom} values of West Kasrik (Mardin) and Bijavar basin (India) phosphorites are consistent with those of this study (İmamoğlu et al. 2009; Khan et al. 2012b; Ghasemian et al. 2022). Additionally, trace element mobility and concentration indicate the abundance of Mo, V, Y, Cr and Zn. The enrichment in transition metals in apatites was interpreted to be mediated by the continental flow in the sedimentary basin. The abundance of transition metals such as Ni, Co, Cr, Cu, Zn, and V was believed to have resulted from the enrichment induced by the introduction of hydrothermal or mafic volcanic sediments. The high Y/Ho, Ni/Co, V/(V + Ni) and V/Ni ratios of the phosphorites seem to be explained by the presence of transition metals that reveal geochemical contamination, and this situation developed due to paleotectonic events associated with the Tethys Ocean.

In general, positive Eu anomalies indicate that the physicochemical conditions of the environment were reducing. Similar results were obtained from phosphorite deposits in different areas (Bau et al. 2010; Khan et al. 2012a, b; Kechiched et al. 2020). Positive Eu anom-

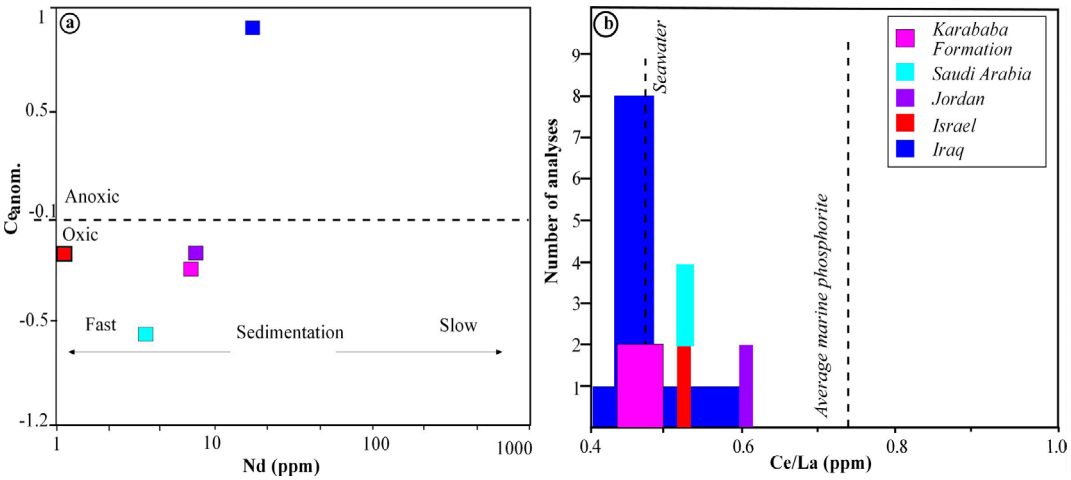

Fig. 12. a) Ceanom.-Nd diagram showing redox conditions as oxic and anoxic environments (Wright et al. 1987); b) Histogram of Ca/La ratios in the Mazıdağı phosphorites (average value, n = 11) (sample No: MMK-3), SW (Høgdahl et al. 1968), AWP (Altschuler 1980), shale (Piper 1974), and other countries

Rys. 12. a) Diagram Ceanom.-Nd przedstawiający warunki redoks w środowisku tlenowym i beztlenowym (Wright i in. 1987); b) Histogram stosunków Ca/La w fosforytach Mazıdağı (wartość średnia, n = 11) (próba nr: MMK-3), SW (Høgdahl i in. 1968), AWP (Altschuler 1980), łupek (Piper 1974), i inne kraje

alies in Mazıdağı apatites indicate the presence of anoxic or suboxic environments in which deep-sea hydrothermal activity was also a factor.

It is known that Ce is rapidly consumed in shallow-water environments, depending on oxidation conditions (Majumdar et al. 2003). Ce anomalies in old marine biogenic phosphorites suggest the presence of oxic conditions in the water column and possibly in the upper pore waters, but the lack of a negative Ce anomaly within biogenic apatite does not necessarily indicate suboxic or anoxic conditions in the water column (Kemp and Trueman 2003). Ce/Ce* data that are substantially greater or lower than 1 imply the presence of Ce^{4+} and therefore oxic conditions

$$(Ce/Ce^* = (Ce_{sample}/Ce_{NASC})/(2/3(La_{sample}/La_{NASC}) + 1/3(Nd_{sample}/Nd_{NASC})$$

(De Baar et al. 1985). The Ce/Ce* values of the phosphorites were between 0.16 and 0.20.

Additionally, with regard to the evaluation of marine environmental conditions, as shown in the included Ce_{anom}–Nd diagram, the phosphorites indicated a rapid sedimentation process that occurred under oxic conditions (Figure 12a). The Ce/La ratios of the apatite samples from Mazıdağı were investigated with the addition of SW (Høgdahl et al. 1968), AWP (Altschuler 1980) and shale (Piper 1974) values (Figure 12b). Phosphorites of the Karababa Formation and from other deposits precisely correlate with the SW composition (Ce/La = 0.35). Moreover, the low Ce/La ratios (between 0.20–0.60) of the Mazıdağı phosphorites and phosphates from other Arabian countries also reflect seawater composition. These results appear to be similar when compared with all other phosphate deposits in the Mediterranean marine phosphate belt.

According to Gallego-Torres et al. (2010), the V/Mo ratio provides information about the redox properties of the depositional medium. V/Mo ratio of anoxic conditions is < 2, whereas this ratio ranges from 2 to 10 in suboxic conditions; however, sediments deposited under in oxic conditions show high V/Mo values (10–60). The V/Mo ratio in phosphorites is between 69.37 and 82.86 and this is above the specified ranges.

The Y/Ho ratio can be used to evaluate the environment in the case of phosphorization. According to Lan et al. (Lan et al. 2019), a value of this ratio higher than 26 indicates that water was frequently contaminated with detrital material. In this study, the Y/Ho ratio values of the samples were determined to be 69.83–71.17, indicating that there were detrital contaminants within the medium. Similarly, some trace elements (Ni, Cr, V, Mo, Cd, Th, U) are markers in determining redox conditions (Morford and Emerson 1999). The relative ratios of these elements (Ni/Co, V/(V+Ni), V/Ni) can be used to demonstrate paleoredox states (Hatch and Leventhal 1992; Jones and Manning 1994). The V/Ni, Ni/Co, and V/(V + Ni) values of the apatite samples were in ranges representing an anoxic environment.

Table 3 shows the comparisons of some trace and rare earth element concentrations from the Cretaceous-Paleocene sedimentary phosphorite deposits on the Arabian and African Plates, as well as other areas. The phosphorites of the Karababa Formation registered trace elements and REEs such as La (16.3 ppm), Sm (1.4 ppm) and V (113.5 ppm), which have not been detected in other countries (Jordan and Morocco) and can result from the high phosphate and carbonate levels (average P_2O_5 35.41 wt.% and CaO 54.80 wt.%). According

Table 3. Some trace element and REE compositions of the average phosphorites in this study in comparison to minerals and reservoirs in different countries

Tabela 3. Niektóre składy pierwiastków śladowych i pierwiastków ziem rzadkich w przeciętnych fosforytach w tym badaniu w porównaniu z minerałami i zbiornikami w różnych krajach

Element ppm	Present study (average, n = 11)	Saudi Arabia[1]	Iraq[2]	Egypt[3]	Jordan[4]	Morocco[5]	AWP	ASC	Soil EC	Fertilizer C.
Ni	8.35	9.6	n.a.	72	15	41.4	53	68	50	180
Zn	206	54.4	150	149	121	279	195	95	200	4,850
Sr	1,512.5	1,228.6	800	1,705	n.a.	1,331	1,900	300	n.a.	n.a.
V	113.5	44.3	120	246	n.a.	n.a.	n.a.	n.a.	n.a.	n.a.
Cr	201.5	4.5	n.a.	161.4	51	217	125	90	60	n.a.
Co	0.95	0.9	n.a.	2.6	n.a.	0.75	7	19	n.a.	150
Mo	1.5	0.7	n.a.	323.4	n.a.	7.9	n.a.	2.5	n.a.	20
As	5.0	6.3	n.a.	19.6	n.a.	10.7	23	13	8	75
Sm	1.39	1.22	20	5.6	n.a.	n.a.	20	n.a.	n.a.	n.a.
La	16.25	12.02	133	33.2	n.a.	n.a.	133	n.a.	n.a.	n.a.
Mn	77	n.a.	n.a.	422	n.a.	15	n.a.	850	n.a.	n.a.
U	55.6	57.3	72	35	n.a.	n.a.	n.a.	n.a.	n.a.	n.a.

n.a. = not available.

[1] Al-Hobaib et al. 2013.

[2] Benni 2013.

[3] Abou El Anwar et al. 2017.

[4] Batarseh and El-Hasan 2009.

[5] Suttouf 2007.

AWP, Average World Phosphorite (Altschuler 1980); ASC, Average Shale Composition (Turekian and Wedelpohl 1961); Soil EC (European Commission EC 1986); Fertilizer Canada (Canadian Food Inspection Agency 1997).

to the Canadian Food Inspection Agency, trace element levels are low compared to other phosphorites from the Middle East and North Africa, such as Jordan and Egypt (Al-Hobaib et al. 2013; Benni 2013) and North African phosphorites (Suttouf 2007), such as those from Egypt (Abou El-Anwar et al. 2017) and Jordan (Batarseh and El-Hasan 2009). Additionally, the Upper Cretaceous Mazıdağı phosphorites in Turkey have rather low levels of average As (5 ppm). These amounts (As) are comparable to those provided by the Canadian Food Inspection Agency (1997) and to standard soil EC values (European Commission EC 1986) but lower than those of AWP (Altschuler 1980). Therefore, the Mazıdağı apatites in the studied area could be appropriate for manufacturing fertilizers. Moreover, the average concentrations of Zn, Sr, and Cr were higher than those in the average shale composition (ASC; Turekian and Wedelpohl 1961). The Ni concentration was lower than those for other countries. Sr, Mo, As, and Mn concentrations were much higher compared to values from all other countries (Table 3). However, U and Co values were similar to those from phosphate minerals from Saudi Arabia (Al-Hobaib et al. 2013).

In marine sedimentary environments, the salinity of seawater is closely related to sedimentation, and it is known that Sr values are directly proportional to salinity. In general, the amount of Sr increases as the salinity of the seawater increases. In this study, the Sr values of the apatite minerals indicated a seawater composition with an average value of 1512 ppm. Sr values have been shown to be similar in studies performed on contemporaneous formations in the Arabian and African Plates, except for those in Iraq and ASC (Table 3).

Conclusions

1. The Karababa Formation is divided into the Karataş, Ekinciler, and Evciler members, which represent different lithofacies, and it has been suggested that lithological, mineralogical and geochemical changes may be criteria for distinguishing the environmental conditions of the basin (depth, nutrient load, biological activity), sedimentation and subsequent weathering/decomposition processes.
2. Apatite-type phosphate and palygorskite/sepiolite-type clay mineral formations observed in different members of the Karababa Formation consist of chemical deposits from the paleomarine environment. Optical microscopy (OM) and SEM investigations show that palygorskite and sepiolite minerals develop authigenically within rock pores. The layers of mixed minerals are formed by neoformation and/or transformation processes, while smectite minerals present in the matrix represent authigenic components. According to the data obtained here, all rock and phyllosilicate/clay mineralogical differences observed in the lithological members of the Upper Cretaceous Karababa Formation were determined to have been related to the tectonic movements of the basin during the Cretaceous period and mineral formation processes.
3. According to the XRD-WR results, the phosphate minerals in the Karataş phosphorite member are composed of carbonate fluorapatite (CFA = $Ca_5(PO_4)_3F$). This is the first

time that CFA minerals (found in peloidal phosphorite rocks) were identified in phosphate-containing rocks in Turkey.

4. The major and trace elements found in the Upper Cretaceous Mazıdağı phosphorites include P_2O_5 (35.19–35.62 wt.%), REEs (44.44–44.69 ppm), Y (50.9–54.8 ppm), and U (5.2–5.7 ppm). According to the results of the geochemical analyses, the apatite minerals detected in the Karababa Formation had high amounts of P_2O_5 (average: 35.41 wt.%), which has significant potential for applications as industrial material.
5. The low Ce_{anom}, Ce/La, and Fe_2O_3 values were related to the shallow oxidation environment where the Karababa phosphorites formed. The petrographic, mineralogical and geochemical analyses suggested that the Upper Cretaceous phosphorite in the Karababa Formation was deposited under shallow slightly oxidizing conditions. The minerals were affected by chemical and mechanical processes in a highly productive environment.

REFERENCES

Aba-Hussain et al. 2009 – Aba-Hussain, A.A., Al-Bassam, K.S. and Al-Rawi, Y.T. 2009. Rare earth elements geochemistry of some Paleocene carbonate fluorapatites from Iraq. *Iraqi Bulletin of Geology and Mining* 6(1), pp. 81–94.

Abed, A.M. 2013. The eastern Mediterranean phosphorite giants: an interplay between tectonics and upwelling. *GeoArabia* 18, pp. 67–94, DOI: 10.2113/geoarabia180267.

Abed et al. 2016 – Abed, A.M., Jaber, O., Alkuisi, M. and Sadaqah, R. 2016. Rare earth elements and uranium geochemistry in the Al-Kora phosphorite province, Late Cretaceous, northwestern Jordan. *Arabian Journal of Geosciences* 9, DOI: 10.1007/s12517-015-2135-6.

Abou El-Anwar et al. 2016 – Abou El-Anwar E.A, Mekky, H.S., Abd El Rahim, SH. and El-Sankary, M.M. 2016. Mineralogical and petrographical study of the Duwi Formation Phosphorite. *Bulletin of the National Research Centre* 41(1), pp. 359–370.

Abou El-Anwar et al. 2017 – Abou El-Anwar, A.A., Mekky, H.S., Abd El Rahim, S.H. and Aita, S.K. 2017. Mineralogical, geochemical characteristics and origin of Late Cretaceous phosphorite in Duwi Formation (Geble Duwi Mine), Red Sea region, Egypt. *Egyptian Journal of Petroleum* 26(1), pp. 157–169, DOI: 10.1016/j.ejpe.2016.01.004.

Acmelab 2023. [Online] http://www.acmelab.com/ [Accessed: 2023-05-04].

Al-Bassam et al. 2010 – Al-Bassam, K.S., Aba-Hussain, A.A., Mohammed, A.Q. and Al-Rawi, Y.T. 2010. Petrographic Classification of Phosphate Components of East Mediterranian Phosphorite Deposits. *Iraqi Bulletin of Geology and Mining* 6(1), pp. 59–79.

Al-Hobaib et al. 2013 – Al-Hobaib, A.S., Baioumy, H.M. and Al-Ateeq, M.A. 2013. Geochemistry and origin of the Paleocene phosphorites from the Hazm Al-Jalamid area, northern Saudi Arabia. *Journal of Geochemical Exploration* 132, pp. 15–25, DOI: 10.1016/j.gexplo.2013.04.001.

Almogi-Labin et al. 1993 – Almogi-Labin, A., Bein, A. and Sass, E. 1993. Late Cretaceous upwelling system along the southern Tethys margin (Israel): interrelationship between productivity, bottom water environments, and organic matter preservation. *Paleoceanography 8*(5), pp. 671–690, DOI: 10.1029/93PA02197.

Altschuler, Z.S. 1980. The geochemistry of trace elements in marine phosphorites. Part I. Characteristic abundances and enrichment, In Bentor, Y.K. (ed.), Marine Phosphorites. *SEPM Special Publication* 29, pp. 19–30, DOI: 10.2110/pec.80.29.0019.

Altschuler et al. 1967 – Altschuler, Z.S., Berman, S. and Cuttita, F. 1967. Rare earths in phosphorites geochemistry and potential recovery. U.S. Geol. Suro., Prot. Pap. (United States), 575-B: B1.

Alvarez et al. 1980 – Alvarez, L.W., Alvarez, W. and Asaro, F. 1980. Extraterrestrial cause for the Cretaceous-Tertiary extinction. *Science* 208(4448), pp. 1095–1110, DOI: 10.1126/science.208.4448.1095.

Ames, L.L. 1959. The genesis of carbonate apatites. *Economic Geology* 54(5), pp. 829–841, DOI: 10.2113/gsecongeo.54.5.829.

Amine et al. 2009 – Amine, M., Asafar, F., Bilali, L. and Nadifiyine, M. 2019. Hydrochloric acid leaching study of rare earth elements from Moroccan phosphate. *Journal of Chemistry* 2019, DOI: 10.1155/2019/4675276.

Arning et al. 2009 – Arning, E.T., Birgel, D., Brunner, B. and Peckmann, J. 2009. Bacterial formation of phosphatic laminites off Peru. *Geobiology* 7, pp. 295–307, DOI: 10.1111/j.1472-4669.2009.00197.x.

Arthur, M.A. and Jenkyns, H.C. 1981. Phosphorites and paleooceanography. *Oceanologica Acta* special issue, pp. 83–96.

Baioumy et al. 2007 – Baioumy, H.M., Tada, R. and Gharaie, M.H.M. 2007. Geochemistry of Late Cretaceous phosphorites in Egypt: implication for their genesis and diagenesis. *Journal of African Earth Sciences* 49(1–2), pp. 12–28, DOI: 10.1016/j.jafrearsci.2007.05.003.

Banerjee et al. 2020 – Banerjee, S., Choudhury, T.R., Saraswati, P.K. and Khanolkar, S. 2020. The formation of authigenic deposits during Paleogene warm climatic intervals: a review. *Journal of Palaeogeography* 9(1), pp. 1–27, DOI: 10.1186/s42501-020-00076-8.

Bardet et al. 2000 – Bardet, N., Cappetta, H., Pereda Suberbiola, X., Mouty, M., Al Maleh, A.K., Ahmad, A.M., Khrata, O. and Gannoum, N. 2000. The marine vertebrate faunas from the Late Cretaceous phosphates of Syria. *Geological Magazine* 137(3), pp. 269–290, DOI: 10.1017/S0016756800003988.

Batarseh, M. and El-Hasan, T. 2009. Toxic Element Levels in the Phosphate Deposits of Central Jordan. *Environmental Earth Sciences* 2(2), pp. 81–88, DOI: 10.1080/15320380802660214.

Bau et al. 2010 – Bau, M., Balan, S., Schmidt, K. and Koschinsky, A. 2010. Rare earth elements in mussel shells of the Mytilidae family as tracers for hidden and fossil high-temperature hydrothermal systems. *Earth and Planetary Science Letters* 299(3–4), pp. 310–316, DOI: 10.1016/j.epsl.2010.09.011.

Beer, H. 1966. Geology of phosphate layers around Mardin-Derik-Mazidağı (*Mardin-Derik-Mazıdağı çevresindeki fosfatlı tabakaların jeolojisi*). *Maden Tetkik ve Arama Enstitüsü Dergisi* 66(66), pp. 104–120 *(in Turkish).*

Belayouni, H. and Beja-Sassi, A. 1987. *Excursion guidebook*. 10th International Field Workshop and Symposium: Genesis of the Tethyan phosphorites and associated petroleum source rocks, Tunisia. International Geoscience Program 156, Phosphorites, 131 p.

Benni, T. 2013. Phosphate Deposits of Iraq. In *UNFC Workshop, Santiago de Chile*.

Berker, E. 1972. Türkiye Phosphate Deposits (*Türkiye Fosfat Yatakları*). *Bilimsel Madencilik Dergisi* 11(4), pp. 77–82 *(in Turkish).*

Berker, E. 1989. The Mardin-Mazidagi-Derik phosphate deposits, south-eastern Turkey. [In:] Phosphate deposits of the world. *Phosphate rock resources* pp. 380–386.

Bezzi et al. 2012 – Bezzi, N., Aifa, T., Hamoudi, S. and Merabet, D. 2012. Trace elements of Kef Es Sennoun natural Phosphate (Djebel Onk, Algeria) and how they affect the various Mineralurgic modes of treatment. *Procedia Engineering* 42, pp. 1915–1927, DOI: 10.1016/j.proeng.2012.07.588.

Boggs, S. 2009. *Petrology of Sedimentary Rocks*. 2nd Edition, Cambridge University Press, New York, 600 pp.

Bowles et al. 1971 – Bowles, F.A., Angino, E.A., Hosterman, J.W. and Galle, O.K. 1971. Precipitation of deep-sea palygorskite and sepiolite. *Earth and Planetary Science Letters* 11(1–5), pp. 324–332.

Brindley, G.W. 1980. *Quantitative X-Ray Mineral Analysis of Clay*s. [In:] Brindley, G.W. and Brown, G., eds. *Crystal Structures of Clay Minerals and Their X-Ray Identification* (pp. 411–438). Mineralogical Society, London.

Brindley, G.W. and Brown, G. 1980. *Crystal structures of clay minerals and their X-ray identification*. Mineralogical Society Monograph, No. 5. *Mineralogical Society London* 495 pp.

Brock, J. and Schulz-Vogt, H.N. 2011. Sulfide induces phosphate release from polyphosphate in cultures of a marine Beggiatoa strain. *ISME Journal* 5, pp. 497–506, DOI: 10.1038/ismej.2010.135.

Brown, G. 1961. The X-Ray Identification and Crystal Structures of Clay Minerals. *Mineralogical Society of London (Clay Minerals Group)* 543 pp.

Caillère, S. and Hénin, S. 1963. Minéralogie des Argiles. *Soil Science* 98(3), 208 pp.

Canadian Food Inspection Agency 1997. Plant Production: fertilizers section.

Cater, J.M.L. and Gillcrist, J.R. 1994. Karstic reservoirs of the mid-Cretaceous Mardin Group, SE Turkey: tectonic and eustatic controls on their genesis, distribution and preservation. *Journal of Petroleum Geology* 17(3), pp. 253–278, DOI: 10.1111/j.1747-5457.1994.tb00134.x.

Chahi et al. 1993 – Chahi, A., Duplay, J. and Lucas, J. 1993. Analyses of palygorskites and associated clays from the Jbel Rhassoul (Morocco): Chemical characteristics and origin of formation. *Clays and Clay Minerals* 41(4), pp. 401–411, DOI: 10.1346/CCMN.1993.0410401.

Choquette, P.W. and James, N.P. 1990. Lime stones the burial diagenetic environment, In McIlreath, I.A., and Morrow, D.W. eds. *Diagenesis,* Ottowa, Ontaria, Canada*, Geological Association of Canada* pp. 75–111.

Church, T.M. and Velde, B. 1979. Geochemistry and origin of a deep-sea Pacific palygorskite deposit. *Chemical Geology* 25(1–2), pp. 31–39, DOI: 10.1016/0009-2541(79)90081-0.

Condie, K.C. 1993. Chemical composition and evolution of the upper continental crust: Contrasting results from surface samples and shales. *Chemical Geolog* 104(1–4), pp. 1–37, DOI: 10.1016/0009-2541(93)90140-E.

Cook, P.J. 1972. Petrology and geochemistry of the phosphate deposits of North West Queensland, Australia. *Economic Geology* 67, pp. 1193–1213, DOI: 10.2113/gsecongeo.67.8.1193.

Cook, P. J. and Cook, J.R. 1985. Marine biological change and phosphogenesis around the Cretaceous-Tertiary boundary. *Sciences Géologiques, bulletins et mémoires* 77(1), pp. 105–108.

Cook, P.J. and McElhinny, M.W. 1979. A re-evaluation of the spatial and temporal distribution of sedimentary phosphate deposits in the light of plate tectonic. *Economic Geology* 74(2), pp. 315–330, DOI: 10.2113/gsecongeo.74.2.315.

Couture, R.A. 1977. Composition and origin of palygorskite-rich and montmorillonite-rich zeolite-containing sediments from the Pacific Ocean. *Chemical Geology* 19, pp. 113–130, DOI: 10.1016/0009-2541(77)90009-2.

Crosby, C.H. and Bailey, J.V. 2012. The role of microbes in the formation of modern and ancient phosphatic mineral deposits. *Frontiers in Microbiology* 3, DOI: 10.3389/fmicb.2012.00241.

Çoban, H. 1987. Derik Mazıdağı (Mardin) Fosfat yataklarının Sedimantolojisi (*Yayımlanmamış Yüksek Lisans Tezi*), Ankara Üniversitesi Fen Bilimleri Enstitüsü *(in Turkish).*

Daneshian et al. 2015 – Daneshian, J., Shariati, S. and Salsani, A. 2015. Biostratigraphy and planktonic foraminiferal abundance in the phosphate bearing Pabdeh Formation of the lar mountains (SW Iran). *Neues Jahrbuch* für *Geologie und Paläontologie–Abhandlungen* 278(2), pp. 175–189, DOI: 10.1127/njgpa/2015/0522.

De Baar et al. 1985 – De Baar, H.J.W., Bacon, M.P., Brewer, P.G. and Bruland, K.W. 1985. Rare earth elements in the Pacific and Atlantic Oceans. *Geochimica et Cosmochimica Acta* 49(9), pp. 1943–1959, DOI: 10.1016/0016-7037(85)90089-4.

Douville et al. 1999 – Douville, E., Bienvenu, P., Charlou, J.L., Donval, J.P., Fouquet, Y., Appriou, P. and Gamo, T. 1999. Yttrium and rare earth elements in fluids from various deep-sea hydrothermal systems. *Geochimica et Cosmochimica Acta* 63(5), pp. 627–643, DOI: 10.1016/S0016-7037(99)00024-1.

Dunoyer De Segonzac, G. 1970. The transformation of clay minerals during diagenesis and low-grade metamorphism: a review. *Sedimentology* 15(3–4), pp. 281–346, DOI: 10.1111/j.1365-3091.1970.tb02190.x.

El Bamiki et al. 2021 – El Bamiki, R., Raj, O., Ouabid, M., Elghali, A., Yazami, O. K. and Bodinier, J.-L. 2021. Phosphate Rocks: A Review of Sedimentary and Igneous Occurrences in Morocco. *Minerals* 11(10), DOI: 10.3390/min11101137.

Estéoule-Choux, J. 1984. Palygorskite in the Tertiary deposits of the Armorican Massif. [In:] Palygorskite-Sepiılite: Occurrences, Genesis and Uses. Singer, A. and Galan E. Eds., In *Developments in Sedimentology* Amsterdam Elsevier, 37, pp. 75–85.

European Commission (EC) 1986. Council Directive (86/278/EEC) on the protection of the environment, and in particular of soil, when sewage sludge is used in agriculture. *Official Journal of European Community* L181 (Annex 1A), pp. 6–12.

Folk, R.L. 1962. Spectral subdivision of limestone types*. American Association of Petroleum Geologist Bulletin* 1, pp. 62–84.

Föllmi, K.B. 1996. The phosphorus cycle, phosphogenesis and marine phosphate-rich deposits. *Earth-Science Reviews* 40(1–2), pp. 55–124, DOI: 10.1016/0012-8252(95)00049-6.

Gallala et al. 2016 – Gallala, W., Saïdi, M., El Hajii, S., Zayani, K., Gaied, M.E. and Montacer, M. 2016. Characterization and valorization of Tozeur-Nefta phosphate ore deposit (Southwestern Tunisia). *Procedia Engineering* 138, pp. 8–18, DOI: 10.1016/j.proeng.2016.02.047.

Gallego-Torres et al. 2010 – Gallego-Torres, D., Martinez-Ruiz, F.C., De Lange, G. J., Jiménez-Espejo, F.J. and Ortega-Huertas, M. 2010. Trace-elemental derived paleoceanographic and paleoclimatic conditions for Pleistocene

Eastern Mediterranean sapropels. *Palaeogeography, Palaeoclimatology, Palaeoecology* 293(1–2), pp. 76–89, DOI: 10.1016/j.palaeo.2010.05.001.

Ghasemian et al. 2022 – Ghasemian, S., Öztürk, H. and Cansu, Z. 2022. Geochemistry of red and cream phosphorites from the Şemikan phosphorite deposit, SE Turkey: Implication for phosphorite deposition conditions in the Upper Cretaceous. *Journal of African Earth Sciences* 185, pp. 104–398, DOI: 10.1016/j.jafrearsci.2021.104398.

Goldhammer et al. 2010 – Goldhammer, T., Bruchert, V., Ferdelman, T.G. and Zabel, M. 2010. Microbial sequestration of phosphorus in anoxic upwelling sediments. *Nature Geoscience* 3(8) pp. 557–561, DOI: 10.1038/ngeo913.

Göncüoğlu, M.C. and Turhan, N. 1984. Geology of the Bitlis Metamorphic Belt. *Conference Geology of the Taurus Belt, Ankara, 1*, pp. 237–244 *(in Turkish).*

Göncüoğlu et al. 1997 – Göncüoğlu, M.C., Dirik, K. and Kozlu, H. 1997. General characteristics of pre-Alpine and Alpine Terranes in Turkey: Explanatory notes to the terrane map of Turkey. *Annales Géologiques Des Pays Helléniques* 37, pp. 515–536.

Gromet et al. 1984 – Gromet, L.P., Dymek, R.F., Haskin, L.A. and Korotev, R.L. 1984. The "North American shale composite": its compilation, major and trace element characteristics. *Geochimica et Cosmochimica Acta* 48(12), *pp.* 2469–2482, DOI: 10.1016/0016-7037(84)90298-9.

Handfield et al. 1959 – Handfield, R.W., Bryant, G.F. and Keskin, C. 1959. Measured section, Korudağ (American Overseas Petroleum). *TPAO Search Group* Report No: 523 *(in Turkish).*

Hatch, J.R. and Leventhal, J.S. 1992. Relationship between inferred redox potential of the depositional environment and geochemistry of the Upper Pennsylvanian (Missourian) Stark Shale Member of the Dennis Limestone, Wabaunsee County, Kansas, USA. *Chemical Geology* 99(1–3), pp. 65–82, DOI: 10.1016/0009-2541(92)90031-Y.

Hoffman, J. and Hower, J. 1979. Clay mineral assemblages as low grade metamorphic geothermometers: application to the thrust faulted disturbed belt of Montana, USA. [In:] Aspects of Diagenesis, Scholle, P.A. and Schluger P.R. Eds., *The Society of Economic Paleontologists and Mineralogists, Special Publication* 26, pp. 55–79.

Hogdahl et al. 1968 – Hogdahl, O. T., Welsom, S. and Bowen, V. T. 1968. Neutron activation analysis of lanthanide elements in sea water. *Advances in Chemistry* 73, pp. 308–325.

İmamoğlu et al. 2009 – İmamoğlu, Ş., Nathan, Y., Çoban, H., Soudry, D., and Glenn, C. 2009. Geochemical, mineralogical and isotopic signatures of the Semikan. West Kasrık Turkish phosphorites from the Derik–Mazıdağı–Mardin area, SE Anatolia. *International Journal Earth Science* 98, pp. 1679–1690, DOI: 10.1007/s00531-008-0332-1.

Isphording, W.C. 1984. The clays of Yucatan, Mexico; a contrast in genesis: Singer, A. and Galan, E. eds., Palygorskite-Sepiolite Occurrences, Genesis and Uses. *Developments in Sedimentology* 37, pp. 59–73.

Jarvis, I. 1992. Sedimentology, geochemistry and origin of phosphatic chalk: The Upper Cretaceous of NW Europe. *Sedimentology* 39, pp. 55–97, DOI: 10.1111/j.1365-3091.1992.tb01023.x.

Jarvis et al. 1994 – Jarvis, I., Burnett, W.C., Nathan, Y., Almbaydin, F.S.M., Attia, A.K.M., Castro, L.N. and Zanin, Y.N. 1994. Phosphorite geochemistry: state-of-the-art and environmental concerns. *Eclogae Geologicae Helvetiae* 87(3), pp. 643–700.

J.C.P.D.S. 1990. *Powder Diffraction File*. Alphabetical Indexes Inorganic Phases. Swarthamore, U.S.A.

Jones, B. and Manning, D.A. 1994. Comparison of geochemical indices used for the interpretation of palaeoredox conditions in ancient mudstones. *Chemical geology* 111(1–4), pp. 111–129, DOI: 10.1016/0009-2541(94)90085-X.

Kechiched et al. 2020 – Kechiched, R., Laouar, R., Bruguier, O., Kocsis, L., Salmi-Laouar, S. 2020. Comprehensive REE^{+} Y and sensitive redox trace elements of Algerian phosphorites (Tébessa, eastern Algeria): A geochemical study and depositional environments tracking. *Journal of Geochemical Exploration* 208, pp. 106–396, DOI: 10.1016/j.gexplo.2019.106396.

Kemp, R.A. and Trueman, C.N. 2003. Rare earth elements in Solnhofen biogenic apatite: geochemical clues to the palaeoenvironment. *Sedimentary Geology* 155(1–2), pp. 109–127, DOI: 10.1016/S0037-0738(02)00163-X.

Khan et al. 2012a – Khan, K.F., Shamim Dar, A., Saif, T. and Khan, A. 2012a. Geochemistry of phosphate bearing sedimentary rocks in parts of Sonrai block, Lalitpur District, Uttar Pradesh, India. *Chemie der Erde* 72(2), pp. 117–115, DOI: 10.1016/j.chemer.2012.01.003.

Khan et al. 2012b – Khan, K.F., Shamim Dar, A., Saif, T. and Khan A. 2012b. Rare earth element (REE) geochemistry of phosphorites of the Sonrai area of Paleoproterozoic Bijawar basin, Uttar Pradesh, India. *Journal of Rare Earths* 30(5), pp. 507–514, DOI: 10.1016/S1002-0721(12)60081-7.

Krumbein, W.C. and Garrels, R.M. 1952. Origin and classification of chemical sediments in terms of pH and oxidation-reduction potentials. *The Journal of Geology* 60(1), pp. 1–33.

Lan et al. 2019 – Lan, C.Y., Yang, A.Y., Wang, C.L. and Zhao, T.P. 2019. Geochemistry, U-Pb zircon geochronology and Sm-Nd isotopes of the Xincai banded iron formation in the southern margin of the North China Craton: implications on Neoarchean seawater compositions and solute sources. *Precambrian Research* 326, pp. 240–257, DOI: 10.1016/j.precamres.2017.10.024.

Lauriente, D.H. 1996. *Phosphate industry overview*. [In:] *Chemical Economics Handbook*; SRI International: Zurich, Switzerland, 94 pp.

Lécuyer et al. 2004 – Lécuyer, C., Reynard, B. and Grandjean, P. 2004. Rare earth element evolution of Phanerozoic seawater recorded in biogenic apatites. *Chemical Geology* 204(1–2), pp. 63–102, DOI: 10.1016/j.chemgeo.2003.11.003.

Lucas, J. and Prévôt-Lucas, L. 1996. Tethyan Phosphates and Bioproductites. [In:] Nairn, A.E., Ricou, L.-E., Vrielynck, B. and Dercourt, J. eds., *The Tethys Ocean, Springer, Boston, MA,* pp. 367–391.

Majumdar et al. 2003 – Majumdar, A., Tanaka, K., Takahashi, T. and Kawabe, I. 2003. Characteristics of rare earth element abundances in shallow marine continental platform carbonates of Late Neoproterozoic successions from India. *Geochemical Journal* 37(2), pp. 277–289, DOI: 10.2343/geochemj.37.277.

Mand et al. 2018 – Mand, K., Kirsimae, K., Lepland, A., Crosby, C.H., Bailey, J. V., Konhauser, K.O., Wirth, R., Schreiber, A. and Lumiste, K. 2018. Authigenesis of biomorphic apatite particles from Benguela upwelling zone sediments off Namibia: The role of organic matter in sedimentary apatite nucleation and growth. *Geobiology* 16(6), pp. 640–658, DOI: 10.1111/gbi.12309.

McArthur, J.M. and Walsh, J.N. 1984. Rare-earth geochemistry of phosphorites. *Chemical Geology* 47(3–4), pp. 191–220, DOI: 10.1016/0009-2541(84)90126-8.

Meissner, C.R. and Ankary, A. 1970. *Geology of phosphate deposits in the Sirhan-Turayf Basin, Kingdom of Saudi Arabia*. United States Department of the Interior U.S. Geological Survey Special report, DOI: 10.3133/20095.

Michard et al. 1983 – Michard, A., Albarede, F., Michard, G., Minster, J.F. and Charlou, J.L. 1983. Rare-earth elements and uranium in high-temperature solutions from East Pacific Rise hydrothermal vent field (13 N). *Nature* 303(5920), pp. 795–797.

Millot, G. 1970. *Geology of Clays: weathering, sedimentology, geochemistry.* Springer Science & Business Media, 429 pp.

Moore, D.M. and Reynolds, R.C. 1997. *X-Ray Diffraction and the Identification and Analysis of Clay Minerals*. Oxford University Press 332 pp.

Morford, J.L. and Emerson, S. 1999. The Geochemistry of Redox Sensitive Trace Metals in Sediments. *Geochimica et Cosmochimica Acta* 63, pp. 1735–1750, DOI: 10.1016/S0016-7037(99)00126-X.

Nathan, Y. and Sass, E. 1981. Stability relations of apatites and calcium carbonates. *Chemical Geology* 34(1–2), pp. 103–111.

Nathan, Y. and Soudry, D. 2018. Authigenic silicate minerals in phosphorites of the Negev, Southern Israel. *Clay Minerals* 17(2), pp. 249–254, DOI: 10.1180/claymin.1982.017.2.10.

Okay, A. I. 2008. Geology of Turkey: a synopsis. *Anschnitt* 21, pp. 19–42.

Orris, G. and Chernoff, C.B. 2004. Review of world sedimentary phosphate deposits and occurrences. Chapter 20. [In:] Hein, J.R., eds. Life cycle of the Phosphoria Formation, Handbook of Exploration and Environmental Geochemistry. *Elsevier Science B.V*.

Owen, R.M. and Olivarez, A.M. 1988. Geochemistry of rare earth elements in Pacific hydrothermal sediments. *Marine Chemistry* 25(2), pp. 183–196, DOI: 10.1016/0304-4203(88)90063-1.

Panczer et al. 1989 – Panczer, G., Nathan, Y. and Shiloni, Y. 1989. Trace element characterization of phosphate nodules in Israel. Caractérisation en éléments traces de nodules de phosphate d'Israël. *Sciences Géologiques, Bulletins et Mémoires* 42(3), pp. 173–184.

Perinçek, D. 1980. Sedimentation on the Arabian Shelf under the Control of Tectonic Activity in Taurid Belt. *5th Petroleum Congress of Turkey-Ankara,* pp. 77–93 *(in Turkish).*

Picard et al. 2002 – Picard, S., Lécuyer, C., Barrat, J.A., Garcia, J.P., Dromart, G. and Sheppard, S.M. 2002. Rare earth element contents of Jurassic fish and reptile teeth and their potential relation to seawater composition (Anglo-Paris Basin, France and England). *Chemical Geology* 186(1), pp. 1–16, DOI: 10.1016/S0009-2541(01)00424-7.

Piper, D.Z. 1974. Rare earth elements in ferromanganese nodules and other marine phases. *Geochimica et Cosmochimica Acta* 38/7, pp. 1007–1022, DOI: 10.1016/0016-7037(74)90002-7.

Piper, D.Z. 1999. Trace elements and major-element oxides in the Phosphoria Formation at Enoch Valley, Idaho; Permian sources and current reactivities (No. 99–163). *US Geological Survey.*

Powell, J. 1989. Stratigraphy and sedimentation of the Phanerozoic rocks in central and southern Jordan, part B: Kurnub, Ajlun and Belqa Group. Bulletin 11, *Natural Resources Authority* Jordan, 130 pp.

Salsani et al. 2020 – Salsani, A., Amini, A., Shariati, S., Aghanabati, S. A. and Aleali, M. 2020. Geochemistry, facies characteristics and palaeoenvironmental conditions of the storm-dominated phosphate-bearing deposits of eastern Tethyan Ocean; A case study from Zagros region, SW Iran. *AIMS Geosciences* 6(3), pp. 316–354, DOI: 10.3934/geosci.2020019.

Shields, G. and Stille, P. 2001. Diagenetic constraints on the use of cerium anomalies as palaeoseawater redox proxies: an isotopic and REE study of Cambrian phosphorites. *Chemical Geology* 175(1–2), pp. 29–48.

Singer, A. 1979. Palygorskite in sediments: detrital, diagenetic or neoformed. A critical review. *Geologische Rundschau* 68, pp. 996–1008, DOI: 10.1007/BF01820193.

Singer, A. 1984. Pedogenic palygorskite in the arid environment.in Palygorskite Sepiolite. Occurrences, Genesis and Uses, Singer, A. and Galan E., eds. *Developments in Sedimentology*, 37, Elsevier, pp. 169–176

Singer et al. 1984 – Singer, A. and Galan, E. 1984. Palygorskite-Sepiolite: Occurrences, Genesis and Uses. Amsterdam, Elsevier, *Developments in Sedimentology* 37, 352 pp.

Slansky et al. 1959 – Slansky, M., Camez, T. and Millot, G. 1959. Sedimentation argileuse et phosphatee au Dahomey. *Bulletin de la Société Géologique de France* 7(2), pp. 150–155.

Soudry et al. 2002 – Soudry, D., Ehrlich, S., Yoffe, O. and Nathan, Y. 2002. Uranium oxidation state and related variations in geochemistry of phosphorites from the Negev (southern Israel). *Chemical Geology* 189(3–4), pp. 213–230, DOI: 10.1016/S0009-2541(02)00144-4.

Soudry et al. 2006 – Soudry, D., Glenn, C.R., Nathan, Y., Segal, I. and Vonder Haar, D.L. 2006. Evolution of Tethyan phosphogenesis along the northern edges of the Arabian-African shield during the Cretaceous-Eocene as deduced from temporal variations of Ca and Nd isotopes and rates of P accumulation. *Earth Science Reviews* 78(1–2), pp. 27–57, DOI: 10.1016/j.earscirev.2006.03.005.

Srodon, J. 1999. Use of clay minerals in reconstructing geological processes: Recent advances and some perspectives. *Clay Minerals* 34(1), pp. 27–37, DOI: 10.1180/000985599546046.

Suttouf, M. 2007. *Identifying the origin of rock phosphates and phosphorus fertilisers using isotope ratio techniques and heavy metal patterns*. Von der Fakultat fur Lebenswissenschaften der Technischen Universitat Carolo-Wilhelmina, Doktors der Naturwis-senschaften, 196 pp.

Svoboda, K. 1989. The lower Tertiary phosphate deposits of Tunisia. [In:] Notholt, A.J.G., Sheldon R.P. and Davidson, D.F., eds. Phosphate Deposits of the World, Volume 2, Phosphate Rock Resources. *Cambridge University Press*, pp. 284–288.

Tlili et al. 2010 – Tlili, A., Felhi, M. and Montacer, M. 2010. Origin and depositional environment of palygorskite and sepiolite from the Ypresian phosphatic series, Southwestern Tunisia. *Clays and Clay Minerals* 58(4), pp. 573–584, DOI: 10.1346/CCMN.2010.0580411.

Torres-Ruiz et al. 1994 – Torres-Ruiz, J., Lopez-Galindo, A., Gonzalez, L. and Delgado Huertas, A. 1994. Geochemistry of Spanish sepiolite/palygorskite deposits: Genetic consideration; based on trace elements and isotopes. *Chemical Geology* 112, pp. 221–245, DOI: 10.1016/0009-2541(94)90026-4.

Turekian, K.K. and Wedelpohl, K.H. 1961. Distribution of the Elements in Some Major Units of the Earth's Crust. *Geological Society of America Bulletin* 2, pp. 175–192, DOI: 10.1130/0016-7606(1961)72[175:DOTEIS]2.0.CO;2.

Umut, M. 2011. 1/100.000 ölçekli Türkiye Jeoloji Haritası, Diyarbakır N 44 paftası. Maden Tetkik ve Arama Genel Müdürlüğü Yayınları, Ankara *(in Turkish).*

Varol, B. 1989. Mazıdağ-Derik (Mardin) fosfat pelloidlerinin sedimanter petrografisi ve kökeni. *Maden Tetkik ve Arama Dergisi* 109, pp. 119–126 *(in Turkish).*

Weaver, C.E. 1984. Origin and geologic applications of the palygorskite deposits of the S. E. United States. [In:] Singer, A. and Galan, E., eds. Palygorskite-Sepiolite: Occurrences, Genesis and Uses, *Developments in Sedimentology Amsterdam*, Elsevier 37, pp. 39–58.

Wright et al. 1987 – Wright, J., Schrader, H. and Holserab, W.T. 1987. Paleoredox variations in ancient oceans recorded by rare earth elements in fossil apatite. *Geochimica et Cosmochimica Acta* 51(3), pp. 631–644, DOI: 10.1016/0016-7037(87)90075-5.

Yalçın, H. and Bozkaya, Ö. 1995. Sepiolite-palygorskite from the Hekimhan region (Turkey) − *Clays and Clay Minerals* 43, pp. 705–717, DOI: 10.1346/CCMN.1995.0430607.

Yılmaz et al. 2018 – Yılmaz, I.O., Cook, T.D., Hoşgör, I., Wagreich, M., Rebman, K. and Murray, A.M. 2018. The upper Coniacian to upper Santonian drowned Arabian carbonate platform, the Mardin–Mazıdağı area, SE Turkey: sedimentological, stratigraphic, and ichthyofaunal records. *Cretaceous Research* 84, pp. 153–167, DOI: 10.1016/j.cretres.2017.09.012.

Yılmaz, Y. 1993. New evidence and model on the evolution of the southeast Anatolian orogeny. *Geological Society of American Bulletin* 105*,* pp. 251–271, DOI: 10.1130/0016-7606(1993)105<0251:NEAMOT>2.3.CO;2.

Yılmaz, Y. 2019. Southeast Anatolian Orogenic Belt revisited (geology and evolution). *Canadian Journal of Earth Sciences* 56, pp. 1163–1180, DOI: 10.1139/cjes-2018-0170.

Zarasvandi et al. 2021 – Zarasvandi, A., Fereydouni, Z., Alizadeh, B., Absar, N., Shukla, A.D., Raza, M.Q., Ashok, M. and Zentilli, M. 2021. Phosphogenesis in the Zagros fold-thrust belt, Iran: The link between the Tethyan paleoenvironment and phosphate ore deposition. *Ore Geology Reviews* 139, DOI: 10.1016/j.oregeorev.2021.104563.

MINERALOGY AND GEOCHEMISTRY OF UPPER CRETACEOUS MAZIDAĞI PHOSPHORITE DEPOSITS FROM THE NORTHERN ARABIAN PLATE (MARDIN, TURKEY)

Keywords

cerium anomalies, Karababa formation, phosphate, rare earth element

Abstract

In the Mardin-Mazıdağı region, which corresponds to the northern Arabian Plate, layers containing marine phosphorite rocks are found within the Karababa Formation (Upper Cretaceous). The Karataş member contains phosphorites and carbonate rocks with nodular chert geodes and fossils.

The phosphorite and micritic limestones contain invertebrate fossil fragments and materials such as optical isotropic pelletic apatite minerals, angular/subangular and plated fish bone fragments, and brachiopod shells. SEM (scanning electron microscopy) results show that the apatite minerals are either spherical or ellipsoidal in shape and their size varies between 100–200 µm. According to X-ray diffraction (XRD) examinations, the rocks contain apatite (carbonate rich fluorapatite; CFA), carbonate (calcite, dolomite), silica (quartz and opal-CT), little feldspar, and clay (smectite, palygorskite/sepiolite, kaolinite, illite, chlorite, mixed layered chlorite-vermiculite (C-V) and illite-vermiculite (I-V).

The average major and trace elements found in the phosphorite include P_2O_5 (35.41 wt.%), REEs (44.57 ppm), Y (52.85 ppm), and U (5.45 ppm). The Mazıdağı phosphorite analysis indicates that the conditions are slightly oxic, which is supported by their slightly negative Ce_{anom} average values

(–0.30), low Ce/La ratios (0.32), and a V/(V + Ni) mean of 0.93 ppm. All the recoded values of the average REE for the study area are considerably lower than those in Iraq (84.30 ppm), Tunisia (400.3 ppm), Morocco (571.75 ppm) and Jordan (187 ppm). It is inferred that mineral formation processes are affected by the biogenic and biogeochemical activities that occurred in conjunction with the changes in sea level driven by the tectonic conditions associated with the evolution of the Neotethys Ocean.

MINERALOGIA I GEOCHEMIA GÓRNOKREDOWYCH ZŁÓŻ FOSFORYTÓW MAZIDAĞI Z PŁYTY PÓŁNOCNO-ARABSKIEJ (MARDIN, TURCJA)

Słowa kluczowe

anomalie ceru, formacja Karababa, fosforyty, pierwiastki ziem rzadkich (REE)

Streszczenie

W regionie Mardin-Mazıdağı, który odpowiada północnej płycie arabskiej, w formacji Karababa (górna kreda) znajdują się warstwy zawierające morskie skały fosforytowe. Jednostka Karataş zawiera fosforyty i skały węglanowe ze sferoidalnymi geodami czertów (konkrekcji) i skamieniałościami.

Wapienie fosforytowe i mikrytyczne zawierają skamieniałe fragmenty bezkręgowców i materiały takie jak: optycznie izotropowe granulowane minerały apatytowe, kanciaste/nieco kanciaste i blaszkowate fragmenty kości ryb oraz muszle ramienionogów. Wyniki SEM (skaningowej mikroskopii elektronowej) pokazują, że minerały apatytu mają kształt kulisty lub elipsoidalny, a ich wielkość waha się między 100–200 µm. Według badań dyfrakcji rentgenowskiej (XRD) skały zawierają apatyt (fluoroapatyt bogaty w węglany; CFA), węglan (kalcyt, dolomit), krzemionkę (kwarc i opal-CT), niewiele skalenia i glinę (smektyt, palygorskit/sepiolit), kaolinit, illit, chloryt, mieszany warstwowy chloryt-wermikulit (C-V) i illit-wermikulit (I-V).

Główne i śladowe pierwiastki występujące w fosforynie zawierają średnio P_2O_5 (35,41% wag.), REE (44,57 ppm), Y (52,85 ppm) i U (5,45 ppm). Analiza fosforytów Mazıdağı wskazuje, że warunki są lekko tlenowe, co potwierdzają ich nieco ujemne średnie wartości Ceanom (–0,30), niski stosunek Ce/La (0,32) i średnia V/(V + Ni) wynosząca 0,93 ppm. Wszystkie zarejestrowane wartości średnie REE dla badanego obszaru są znacznie niższe niż w Iraku (84,30 ppm), Tunezji (400,3 ppm), Maroku (571,75 ppm) i Jordanii (187 ppm). Wywnioskowano, że na procesy formowania się minerałów mają wpływ działania biogenne i biogeochemiczne, które wystąpiły w połączeniu ze zmianami poziomu morza spowodowanymi warunkami tektonicznymi związanymi z ewolucją Oceanu Neotetydy.